NUREG/CR-[illegible]
ANL-83-7

NUREG/CR-3167
ANL-83-7

HEAT TRANSFER TO WATER FROM A VERTICAL TUBE BUNDLE UNDER NATURAL-CIRCULATION CONDITIONS

by

M.J. Gruszczynski and R. Viskanta

ARGONNE NATIONAL LABORATORY, ARGONNE, ILLINOIS

Prepared for the Office of Nuclear Regulatory Research
U. S. NUCLEAR REGULATORY COMMISSION
under Interagency Agreement DOE 40-550-75

The facilities of Argonne National Laboratory are owned by the United States Government. Under the terms of a contract (W-31-109-Eng-38) among the U. S. Department of Energy, Argonne Universities Association and The University of Chicago, the University employs the staff and operates the Laboratory in accordance with policies and programs formulated, approved and reviewed by the Association.

MEMBERS OF ARGONNE UNIVERSITIES ASSOCIATION

The University of Arizona
Carnegie-Mellon University
Case Western Reserve University
The University of Chicago
University of Cincinnati
Illinois Institute of Technology
University of Illinois
Indiana University
The University of Iowa
Iowa State University
The University of Kansas
Kansas State University
Loyola University of Chicago
Marquette University
The University of Michigan
Michigan State University
University of Minnesota
University of Missouri
Northwestern University
University of Notre Dame
The Ohio State University
Ohio University
The Pennsylvania State University
Purdue University
Saint Louis University
Southern Illinois University
The University of Texas at Austin
Washington University
Wayne State University
The University of Wisconsin-Madison

Available from

GPO Sales Program
Division of Technical Information and Document Control
U. S. Nuclear Regulatory Commission
Washington, D.C. 20555

and

National Technical Information Service
Springfield, Virginia 22161

DISCLAIMER

DISCLAIMER

NUREG/CR-3167
ANL-83-7

(Distribution
Codes:
R2 and R4)

ARGONNE NATIONAL LABORATORY
9700 South Cass Avenue
Argonne, Illinois 60439

NUREG/CR--3167

DE83 008459

HEAT TRANSFER TO WATER FROM A VERTICAL TUBE BUNDLE UNDER NATURAL-CIRCULATION CONDITIONS

by

M. J. Gruszczynski and R. Viskanta

School of Mechanical Engineering
Purdue University
West Lafayette, Indiana 47907

Manuscript Completed: August 1982
Date Published: January 1983

ANL Subcontract No. 31-109-38-6959

Prepared for the Division of Reactor Safety Research
Office of Nuclear Regulatory Research
U. S. Nuclear Regulatory Commission
Washington, D. C. 20555
under Interagency Agreement DOE 40-550-75

NRC FIN No. A2014

HEAT TRANSFER TO WATER FROM A VERTICAL TUBE BUNDLE UNDER NATURAL CIRCULATION CONDITIONS

by

M.J. Gruszczynski and R. Viskanta

ABSTRACT

The natural circulation heat transfer data for longitudinal flow of water outside a vertical rod bundle are needed for developing correlations which can be used in best estimate computer codes to model thermal-hydraulic behavior of nuclear reactor cores under accident or shutdown conditions. The heat transfer coefficient between the fuel rod surface and the coolant is the key parameter required to predict the fuel temperature. Because of the absence of the required heat trasfer coefficient data base under natural circulation conditions, experiments have been performed in a natural circulation loop. A seven-tube bundle having a pitch-to-diameter ratio of 1.25 was used as a test heat exchanger. A circulating flow was established in the loop, because of buoyancy differences between its two vertical legs. Steady-state and transient heat transfer measurements have been made over as wide a range of thermal conditions as possible with the system. Steady state heat transfer data were correlated in terms of relevant dimensionless parameters. Empirical correlations for the average Nusselt number, in terms of Reynolds number, Rayleigh number and the ratio of Grashof to Reynolds number are given.

NRC
FIN No. Title

A2014 Heat Transfer to Water from a Vertical
Tube Bundle Under Natural Circulation Conditions

TABLE OF CONTENTS

APPENDICES

LIST OF FIGURES

LIST OF TABLES

NOMENCLATURE

NOMENCLATURE

A_f - cross-sectional flow area in components

C_R - constant in effective flow resistance parameter

c_p - specific heat of fluid

D_h - hydraulic diameter

G - mass flow rate in loop

Gr - Grashof number, $g\beta(\bar{T}_w-\bar{T}_{so})D_h^3/\nu^2$

g - gravitational constant

$\bar{h}_o$ - average heat transfer coefficient on the outside of the bundle

k - thermal conductivity of fluid

L_L - length of hot and cold connecting legs

L_s - distance between hot and cold connecting legs

LMTD - logarithmic mean temperature difference

$\overline{Nu}$ - average Nusselt number, $\bar{h}_o D_h/k$

P - pressure

P_s - perimeter of tube bundle for heat transfer

Pr - Prandtl number, $\mu c_p/k$

Q - average heat transfer rate

R - effective flow resistance parameter defined by Eq. (6)

Ra - Rayleigh number, Gr·Pr

Re - Reynolds number, $GD_h/A_f\mu$

s - spatial coordinate measured around the loop

T - temperature

T_a - ambient air temperature

$\bar{T}_C$ - average temperature in the cold connecting leg

NOMENCLATURE

$\bar{T}_D$ - driving temperature difference defined in Eq. (5)

$\bar{T}_H$ - average temperature of the hot connecting leg

T_I - local temperature of working fluid in the heat exchanger

$\bar{T}_{so}$ - average source (water) temperature inside the tubes

$\bar{T}_w$ - average temperature on the outside of the tube wall

U_a - overall heat transfer coefficient for heat losses to the ambient surroundings

U_s - overall heat transfer coefficient to the tube bundle

β - thermal expansion coefficient

μ - dynamic viscosity

ρ_o - reference density of circulating fluid

ρ - density of circulating fluid

EXECUTIVE SUMMARY

This report contains results of work covering steady-state and transient heat transfer for longitudinal flow of water outside a vertical tube bundle (rods) under natural convection circulation conditions. This type of fundamental information is needed for realistic modeling of the thermal-hydraulic behavior of light water nuclear reactors under transient or accident (e.g., TMI-2) conditions. It is also necessary for the development of computer models to simulate a wide range of postulated nuclear reactor accidents in order to gain insight into measures that can be taken to improve reactor safety. Of special importance is the cooling of a degraded core (i.e., TMI-2) and of the primary coolant system when the reactor is operating under transient and natural circulation conditions.

A rectangular natural circulation loop (thermosyphon) was used to measure the average heat transfer coefficients under natural convection conditions of water at atmospheric pressure in a vertical tube bundle. A seven-tube having a pitch-to-diameter tube ratio of 1.25 was used as a test heat exchanger. A circulating flow was established in the loop because of buoyancy differences in its two vertical legs. Steady-state heat transfer measurements were made over a range of thermal conditions. The heat transfer results were correlated in terms of dimensionless parameters that govern fluid flow and heat transfer in the system. The pressure drop around the loop was found to depend on the Reynolds number alone. Laminar forced flow friction factor correlations were found to correlate the total flow resistance in the loop. Heat transfer results were not predicted by laminar forced flow correlations but were found to depend on the Reynolds, Rayleigh, and Prandtl numbers. Empirical correlations for both fluid friction and heat transfer results are presented.

A one-dimensional model was developed and used to predict the transient response of the system (i.e., temperatures and flow rates) owing to changes in thermal conditions. Comparisons of predictions with experimental data are presented for three different transient conditions: a start up, a step increase in heating rate, and a step decrease in heating rate. The model did not correctly predict the early transient response but yielded correct results for the steady-state conditions at the end of the transient.

1. INTRODUCTION

1.1 Background

In natural convection circulation loops (thermosyphons), heat is convected from a heat source to a heat sink as a result of flow that has been established by density differences in different parts of the system. These are encountered both in nature and in numerous industrial applications. Examples of such applications include industrial and power generating equipment, cooling systems of nuclear reactors, passive solar energy collection systems, and geothermal and geophysical processes. A review of thermosyphon technology is available [1], and numerous publications concerned with system dynamics and thermal performance are cited in recent literature surveys [2,3]. In many of the systems of practical interest, the heat source and/or the heat sink are in the form of vertical rod bundles or tubes. In order to model the system performance, one must know the natural convection heat transfer between the vertical rod (tube) bundle and the circulating fluid.

The dynamics and thermal performance of natural circulation loops (systems) has received considerable attention, and recent surveys of literature are available. Past work on these loops has primarily been concerned with dynamic modeling of flow, heat transfer, and thermal performance. However, neither in these surveys nor in the general heat transfer literature were the authors able to find definitive experimental work on convective heat transfer from a vertical tube rod (bundle) under natural circulation conditions. A survey of related work concerned with free convection from a single vertical cylinder (tube) and a vertical plate placed in an infinite volume of fluid is available [4] and need not be repeated here.

The analysis of natural convection flows requires a knowledge of fluid flow and heat transfer characteristics. It is therefore desirable to compare the results with those for forced flow conditions. Results for forced convection longitudinal flows in rod bundle are well documented and cover a wide range or geometric configurations [5]. The analysis of natural convection flows is very complex, and experimental data are nonexistent [4]. The results for natural convection flows are presented for such specific conditions of heat input as a constant heat flux boundary condition, making the correlating parameters only applicable to identical conditions. It is therefore desirable to review the results for forced flow conditions in infinite tube bundle arrays and to compare them with those of finite arrays contained in channels.

Sparrow and Loeffler [6] have presented an analytical solution for longitudinal, fully developed laminar flow between cylinders arranged in triangular and square arrays. The momentum

equation is solved numerically for pressure drop and friction factor as a function of spacing-to-diameter ratios for both types of arrays. The results are reported as a function of the porosity of the channel and not directly as a function of pitch-to-diameter ratio and number of tubes in the channel. The results indicate that for tube bundle arrays with a porosity of 0.55, the friction factor of a triangular array is greater than that of a square array by 13%.

Zarling [7] has solved the momentum equation for longitudinal pressure drop in fully developed laminar flow through a finite rod bundle. Results are presented in the form of friction factor times Reynolds number (f x Re) for rod bundle geometries consisting of a central rod surrounded by four to ten peripheral rods within a containing channel. The results indicate that for a tube bundle array with seven rods, the friction factor is about 7% smaller than that of an infinite triangular array with the same pitch-to-diameter ratio.

Dwyer and Berry [8] have reported the results of a theoretical study for in-line laminar flow through equilateral infinite triangular rod bundles. Solutions for a wide range of pitch-to-diameter ratios are reported. Fully developed temperature profiles for the uniform wall heat flux boundary condition are assumed to determine the rod-average heat transfer coefficients and circumferential variations of wall temperature.

An analysis of combined convection heat transfer in an infinite rod array has been done by Yang [9]. Triangular and square arrays with uniform heat flux at the surface of the rod in the flow direction and uniform surface temperature in the circumferential direction are analyzed for a large range of pitch-to-diameter ratios. The numerical results indicate that the effect of superimposed natural convection is to increase the Nusselt number and the pressure drop. The effect of the superimposed natural convection is expressed in terms of a Grashof-Reynolds number ratio. Also, the circumferential variation of wall heat flux is reduced under the conditions of combined convection.

An extensive review of literature failed to reveal any experimental and analytical results for fluid friction factors or heat transfer coefficients in a vertical bundle of cylindrical rods under natural circulation conditions. This lack of data has provided the motivation for this study.

1.2 Objectives and Scope

The objective of this research was to obtain fluid friction and heat transfer data for the longitudinal flow of water in a vertical rod (tube) bundle under natural circulation conditions. This type of data base is needed for developing predictive models simulating the thermal hydraulic behavior of pressurized water

reactor systems under loss of coolant circulation or normal shutdown conditions. The specific objectives of the research were the following:

- Measure and correlate average heat transfer coefficients for a tube (in a bundle) in vertical, longitudinal natural convection flow at atmospheric pressure and different thermal conditions

- Predict the transient behavior of the natural convection circulation loop and compare it with experimental data

The scope of the research covered both steady-state and transient conditions. Observations and measurements of heating and for rates allowed an evaluation of frictional resistances and heat transfer coefficients for an atmospheric pressure closed loop using water as the fluid. Parameters that control fluid flow and heat transfer from the bundle were varied over as large a range of conditions as possible. Fluid friction and heat transfer data were measured and are reported. The heat transfer data are tabulated, and empirical correlations valid over a limited range of independent parameters are given.

2. EXPERIMENTS

2.1 Experimental Natural Circulation Loop

An existing natural convection circulation loop made of glass, previously used for natural convection boiling-condensation experiments, was modified and instrumented to perform single-phase natural convection experiments with water at atmospheric pressure. Funding limitations required that this loop be used to assemble the experimental apparatus. The two tube bundles were heat exchangers that used water as the working fluid for heat addition to and removal from the system. This type of arrangement was chosen for a number of reasons. The major reason being, it was simple and inexpensive to construct compared with an electrical resistance heating apparatus. Hot water could be used as the energy source, and there would be no need for expensive power supplies and controls. The heat exchangers were made from copper tubes because they could easily be soldered to headers that held them in an array. Also, the high thermal conductivity of copper presented a low thermal resistance to heat transfer through the tube walls. The flow of water through the inside of the tubes could be at sufficiently high velocity compared with the relatively low velocity expected outside the tubes under natural circulation conditions. This made the convective heat transfer resistance outside the tubes the controlling resistance.

A schematic diagram of the experimental loop is illustrated in Figure 1. The rectangular loop consisted of two vertical legs and two horizontal connecting legs. As shown in the schematic, tube bundle #1 served as the heat source, and tube bundle #2 acted as a heat sink. With this configuration, the flow of water inside the loop is clockwise, and both tube bundles act as counterflow heat exchangers. A photograph of the loop, set up for testing, appears in Figure 2. The main components of the apparatus are the glass loop with insulation and support,two copper tube bundles, the heating and cooling fluid system, and the loop instrumentation.

2.1.1 Glass Loop

The loop was constructed from eight pieces of Kimax glass tubing, four straight tubes, and four tees. The dimensions of these components are given in Figure 3. The glass is 4.8 mm thick and has an inside diameter of 7.62 cm. The manufacturer's specifications are: a maximum working gage pressure of 345 kPa, a maximum operating temperature of 230^{o}C , and a maximum sudden temperature change of 95^{o}C .

The straight tubing was joined to the tees, forming a rectangular loop, by six bolt clamps. A 6.35 mm-thick brass plate separated each of the pieces. The plates served as smooth surfaces for O-rings that sealed the loop at these joints. The plates were also used as mounting brackets for thermocouple probes and a transversing dye injecting probe.

Four circular plates were clamped at each of the open ends of the loop to provide support for the tube bundles and, with O-rings, sealed the loop so it could be filled with the working fluid. To facilitate filling the loop, a reservoir was fitted to one of the top circular plates. The reservoir, open to the atmosphere, allowed for thermal expansion of the fluid, thus maintaining the system at a safe pressure during normal operation. A drain plug on one of the bottom plates allowed for water drainage when necessary.

The loop was insulated with two layers each of 1.27 cm-thick Johns-Manville insulation tubing on the vertical and top horizontal tubes. Sections of this tubing could easily be removed for flow visualization. Owens-Corning R-19 Fiberglas insulation was used on the bottom horizontal tubes and the tees. The loop was clamped to and supported by an angle-iron stand with U-bolts around each of the tees.

2.1.2 Tube Bundles

The two tube bundles consisted of an array of copper tubes held by headers at each end. A diagram of each tube bundle array

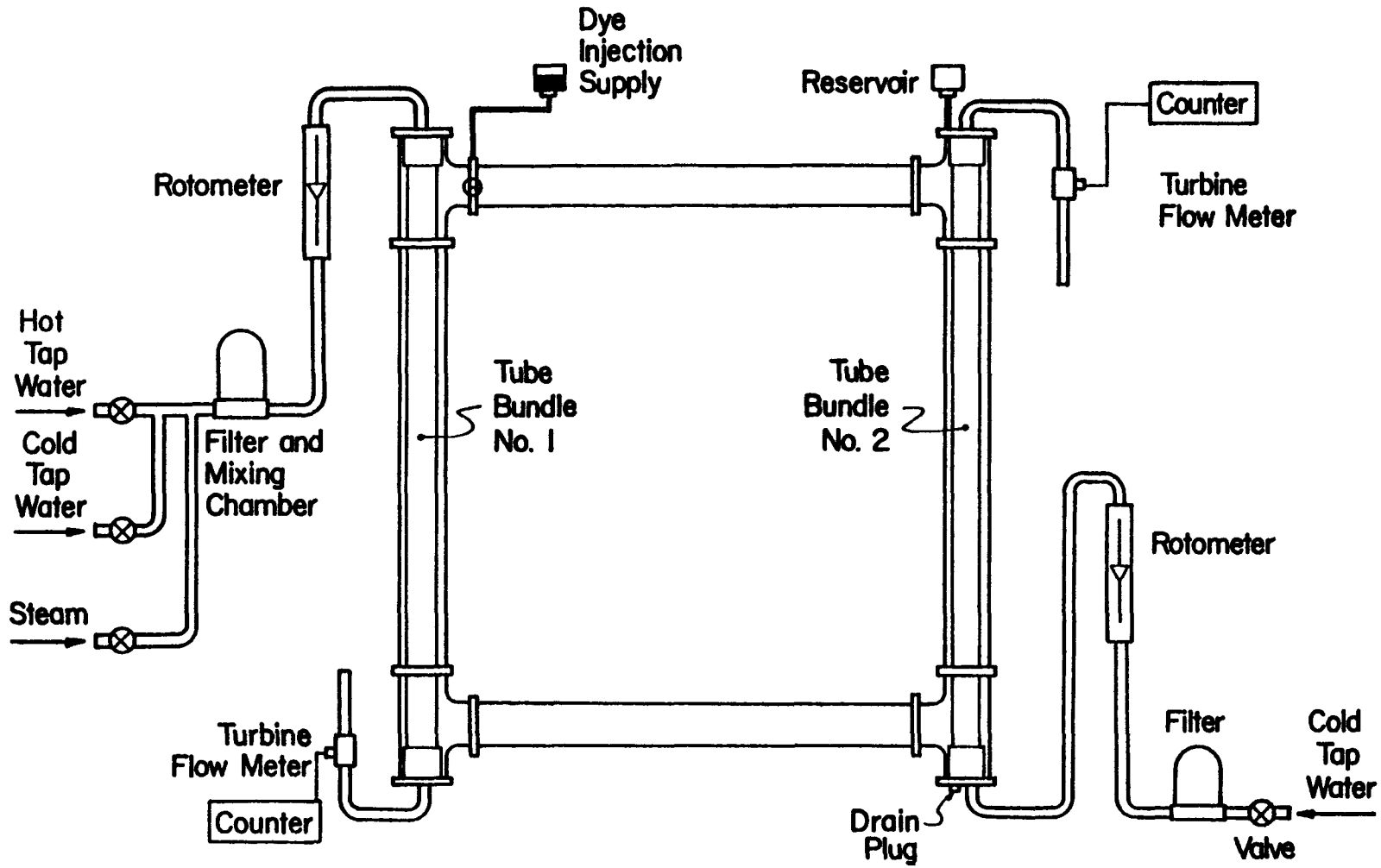

Figure 1. Schematic diagram of the experimental loop.

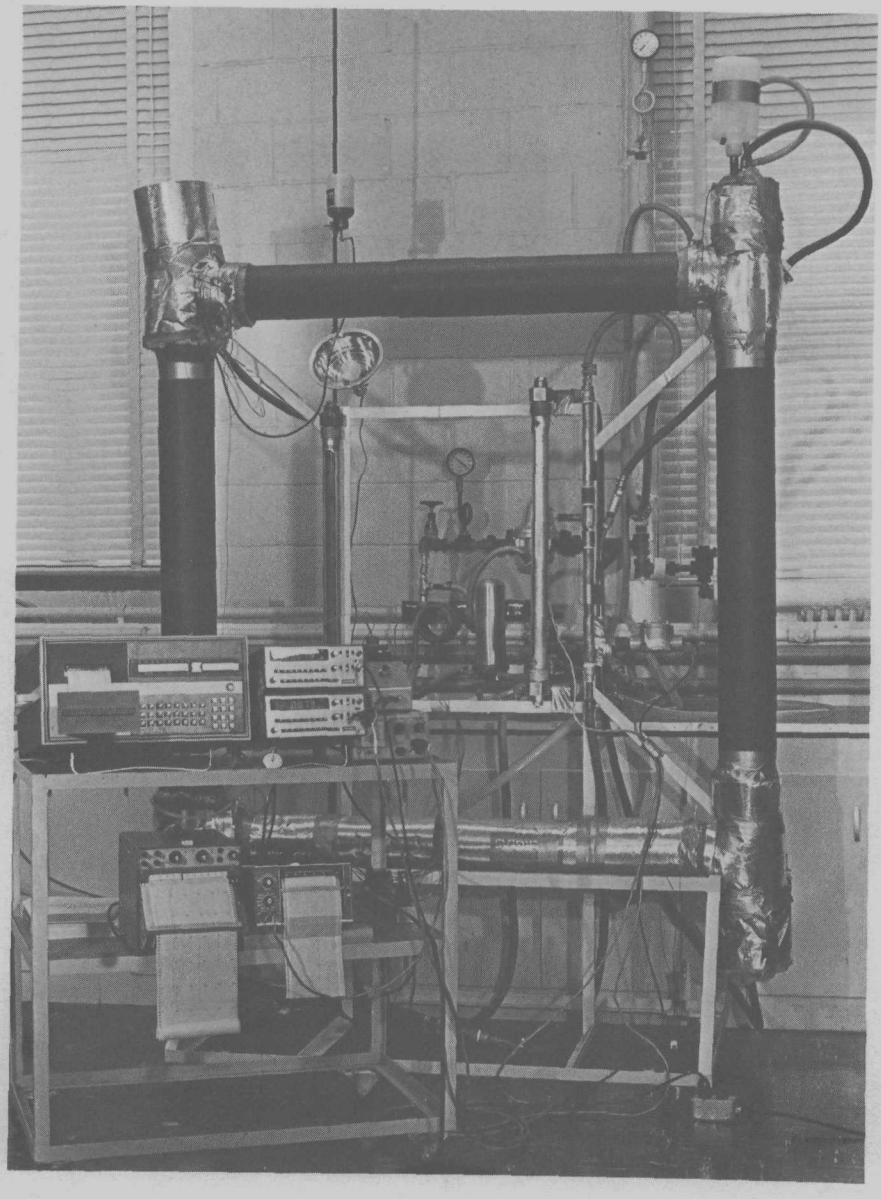

Figure 2. Photograph of the experimental apparatus.

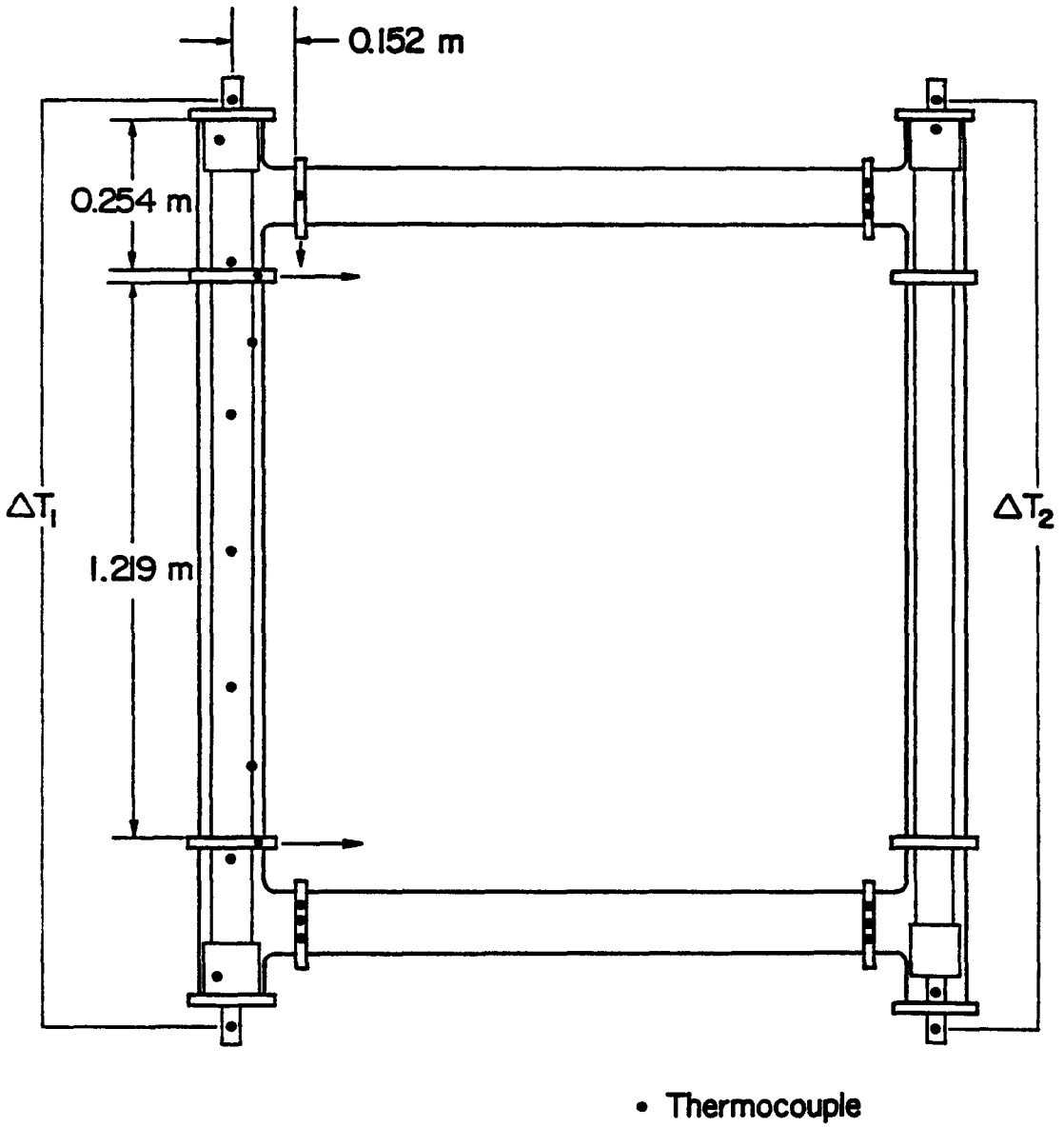

Figure 3. Dimensions of glass loop and thermocouple positions.

is given in Figure 4. The dimensions and characteristics of each tube bundle are given in Table 1. The heat exchanger used to study heat transfer phenomena, tube bundle #1, was a cluster of seven rods arranged in a triangular array with a pitch-to-diameter ratio (PDR) of 1.25. This array was chosen because it is similar to many PWR and LMFBR core bundles. The results for forced flow heat transfer in this type of array are well documented in the literature [5]. The existing heat exchanger,tube bundle #2, contained sixteen tubes. The array pattern of tube bundle #2 was not a regular square or triangular array, so a pitch-to-diameter ratio (PDR) could not be defined.

Both sets of tubes were silver-soldered to the headers to form the heat exchangers. The headers provided support for the arrays and also served as mixing chambers for the heating and cooling fluids. To insure that the water was well mixed and equally distributed among the tubes, the headers of tube bundle #1 were designed with two baffles.

2.1.3 Heating and Cooling Fluid System

Heating and cooling fluid was supplied by cold and hot water lines along with a high pressure steam line. The cooling fluid was supplied by a cold water line at a temperature of $14 \pm 1^{o}C$. To cover as wide range of heat inputs as possible, the heating fluid was supplied by a hot water line mixed with a cold water line and a steam line. A mixing chamber was installed to dampen out flow fluctuations caused by mixing the steam line with the water line. Both fluid lines had filters that prevented particles from clogging the headers of the heat exchangers.

The heating and cooling fluid flow rates could be monitored in two ways. Fisher and Porter rotameters, installed in the fluid lines, measured the instantaneous flow rates of the fluids. However, small flow fluctuations were observed from the float movements. Because of these fluctuations, Brook turbine flow meters were installed in the fluid lines so that average flow rates could be measured. The turbine flow meters produced a number of pulses proportional to the flow rate. The low volume flow meter required a twelve volt DC power supply to transmit the pulses. The pulses were recorded by two Anadex digital counters. The rotometers and turbine flow meters were calibrated prior to use. The calibration curves show that the rotameter readings are dependent on temperature, while the turbine meters are independent of temperature over the calibrated range.

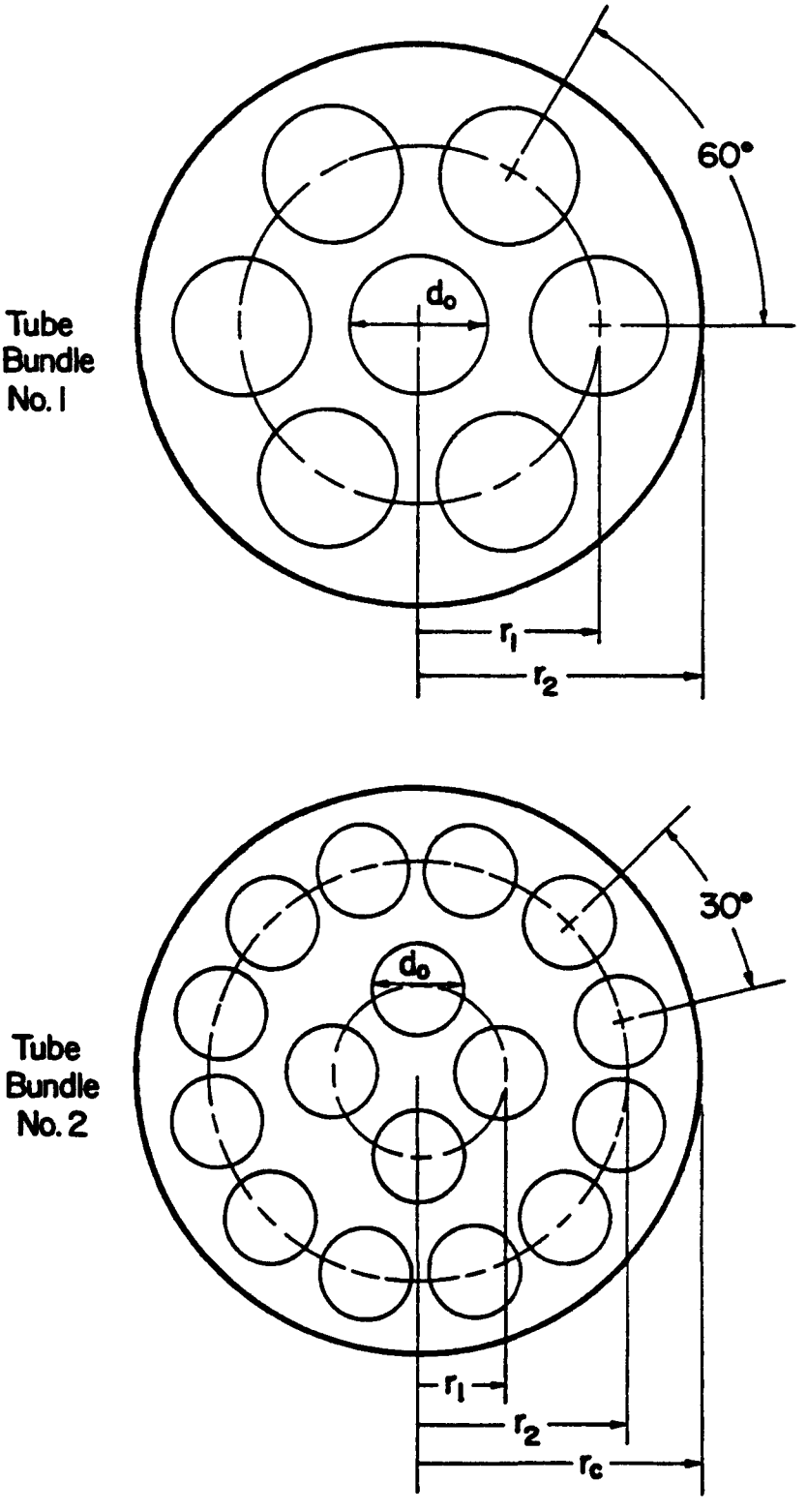

Figure 4. Diagram of tube bundle arrays.

Table 1. Dimensions and Characteristics of the Tube Bundles and Loop

Dimensions	Tube Bundle #1	Tube Bundle #2
No. of tubes	7	16
d_o (m)	0.01905	0.01270
Tube thickness (m)	0.00102	
r_1 (m)	0.002381	0.01111
r_2 (m)		0.02858
r_c (m)	0.03810	0.03810
L_{ht} (m)	1.575	1.524
A_f (m^2)	0.002565	0.002533
ϵ	0.563	0.555
PDR	1.25	
Type of array	Triangular	Mixed
D_H (P_{ht}) (m)	0.0245	0.0159
D_H (P_{sh}) (m)	0.0156	0.0115
D_H(Equiv.flow area)(m)	0.0138	
L_L (m)	1.486	
L_s (m)	1.499	
α (m^{-1})	1869.0	
V (m^3)	0.02145	

2.2 Loop Instrumentation

The heat addition and removal by the heat exchangers was determined from the knowledge of the temperature change across the heat exchangers and the mass flow rate of the fluid through the tubes. Because of the low velocities of the water in the loop, the mass flow rate could not be measured with an orifice or venturi but needed to be determined from an energy balance and a knowledge of the temperatures of the cold and hot connecting legs. The driving temperature difference required to calculate the flow resistance parameters was determined by measuring the temperatures at the ends of the heat exchangers.

The system was instrumented with copper constantan thermocouples. The positions of these thermocouples are given in Figure 3. Seven thermocouples were welded to tube bundle #1 to measure the variation of wall temperature along the tube bundle. Five thermocouples were placed along the outside wall of the central tube, and two were placed on one of the outer tubes. A thermocouple probe was installed at each end of the heat exchangers to measure the temperature of the heating and cooling fluids at these locations. Differential thermocouples were set up across each of the two heat exchangers to accurately measure the heating and cooling fluid temperature difference across the tube bundles.

Monitoring of the fluid inside the loop was restricted to the locations of the brass plates. Three sets of thermocouples were located in the connecting legs. Each set of thermocouples consisted of three individual thermocouples placed across the circular section of the brass plates. These sets of thermocouples gave an average value of the temperature at that section of the of the connecting legs.

A vertical transversing thermocouple probe was installed in the top horizontal connecting leg next to tube bundle #1, This probe could measure the temperature profile across the diameter of the leg at that section of the loop. Two other transversing probes were mounted to the plates in the vertical section of tube bundle #1. These two probes could measure the radial temperature variation through the rod bundle.

Flow visualization was made possible by a horizontally mounted transversing dye injection probe. This probe was mounted on the plate between the top horizontal tube and the tee that contained tube bundle #1. A photograph of this section of the loop, showing the dye probe and thermocouple probe, appears in Figure 8. The probe could be transversed through this section and blue-black dye was supplied by a reservoir.

Temperature measurements of the system were recorded by an Esterline Angus data logger. Continuous temperature readings were recorded with Honeywell and Esterline Angus chart recorders. The copper-constantan thermocouples were connected to an ice bath

reference junction so that millivolt readings could be recorded by the digital averaging option on the Esterline data logger. These readings were changed to degrees Celsius for use in the data reduction.

Measuring the pressure drop of the fluid through the section containing a tube bundle would have required very sensitive instrumentation. Differential pressure readings on the order of one Pascal needed to be measured because of the low velocities in the natural circulation loop.

2.3 Test Procedure

2.3.1 System

The loop was filled with deionized water through the reservoir. The heating fluid line was connected to tube bundle #1 to act as the source; the cooling fluid line was connected to tube bundle #2 as the sink. The direction of the heating or cooling fluid through the tube bundles determined whether they acted as counterflow or parallel-flow heat exchangers. With tube bundle #1 as the source, the flow of fluid in the loop was clockwise, upward around tube bundle #1.

2.3.2 Steady-State Tests

A steady-state condition was reached when all the temperatures monitored showed no change, except for fluctuations, for a period of 5 minutes. A typical steady state test run consisted of fifteen to sixteen readings at different heating rates and lasted approximately nine hours. Initially, the fluid in the loop was at the ambient temperature, with the temperature in the top connecting leg about a degree Celsius higher than in the bottom leg. The flow rates of both the cooling and heating fluids were approximately constant for the test run and were controlled by the valves on the fluid lines. The temperature of the heating fluid was controlled by mixing the cold and hot water lines and the steam line.

The first condition was set with the heating fluid at approximately 20^{o}C at the entrance of the heat exchanger, about 5^{o}C above that of the cooling fluid. The first steady-state readings were taken approximately 1 1/2 hours after start up. Each successive condition was changed by raising the heating fluid approximately 3^{o}C. The test run was concluded when the maximum temperature of the heating fluid was reached.

Readings were recorded and averaged over 5-minute intervals because of temperature and flow rate fluctuations. Thirty temperature readings at ten-second intervals were taken at each condition and averaged by the Esterline data logger. An average

value of the pulses per second from the turbine flow meters was obtained from the total number of pulses over this period of time.

2.3.3. Transient Tests

Transient tests were performed by changing the heating rates to the system. Flow in the loop was initiated by turning on both the heating and cooling fluid lines to the heat exchangers. This first condition was set with heating fluid at approximately 25°C at the entrance of the heat exchanger, about 10°C above that of the cooling fluid. Readings were recorded at one-minute intervals intervals from the start of the transient until a steady-state condition was established in the loop. At this point, steady-state readings were taken.

While the mass flow rate and the inlet temperature of the cooling fluid were kept constant, the temperature of the heating fluid was raised by approximately 20°C at the same flow rate. Reading at this second steady state were taken, and then the heating fluid was lowered to the initial temperature of 25°C . Readings were again recorded every minute until a steady-state condition was established in the loop.

2.4 Data Reduction Procedure

The mass flow rate throu the loop was determined from the energy balances on tube bundle #1 and #2. The two flow rates determined in this manner agreed with each other better than within 10%. This finding is consistent with the calculated heat losses to the ambient enrvironment, which showed that the difference between the heat added by the source and the heat removed by the sink was usually less than 10% of the heat addition to the system.

The average heat transfer coefficient on the outside of the tubes was determined from the definition

$$\bar{h}_o \equiv Q_{so}/A_{ht}\ (\bar{T}_w - \bar{T}_{so}) \qquad (1)$$

The average temperature on the outside of the tube wall $\bar{T}_w$ was determined from the measured temperatues by curve fitting the experimental data and determining the average value. Heat exchanger analysis [9] was used to calculate the local fluid temperature along test bundle #1. From this the average water temperature $\bar{T}_{so}$ was determined.

3. ANALYSIS

3.1 Basic Assumptions

As is customary in the literature [2,3], the basic conservations--the continuity, momentum, and energy equations--are averaged over the cross section normal to the flow direction so only that only the space coordinate s varies clockwise along the loop. The flow is assumed to be laminar, and the density of the circulating fluid is considered to be constant, except in the buoyancy-producing term of the momentum equation, where it is assumed to vary linearly with temperature (Boussinesq approximation). The thermophysical properties of the fluid are evaluated at the average temperature of each system component. Kinetic and potential energy changes of the fluid, heat conduction in the fluid and structural components, and viscous heat dissipation are neglected in comparison with advection. The heat capacity of the structural components (tube bundle, containing loop, insulation) are also neglected in comparison with that of the circulating fluid.

3.2 Mathematical Model

From the equation of conservatin of mass for one-dimensional, incompressible flow, we conclude that the mass flow rate of the circulating fluid in each component of the system is only a function of time,

$$G(t) = f(t) \tag{2}$$

The conservation of momentum law for the legs may be expressed in terms of the mass flow rate, $G = \rho A_f \bar{u}$, and results in the following equation:

$$\frac{1}{A_f}\frac{\partial G}{\partial t} = -\frac{\partial P}{\partial s} \pm \rho_o g[1 - \beta(T-T_o)]fG^2/2\rho D_h A_f \tag{3}$$

The buoyancy force, the second term on the right-hand side of Eq. (3), vanishes for the two horizontal connecting legs.

The energy equation for four components of the loop can be written as

$$\rho c_p \left[A_f \frac{\partial T}{\partial t} + \frac{1}{\rho} \frac{\partial (GT)}{\partial s}\right] = U_s(T_I - T)P_s - U_a(T - T_a)P_a \qquad (4)$$

where U_s and U_a are the overall heat transfer coefficients between the working and circulating fluids and between the circulating fluid and the ambient surroundings, respectively. Of course, the first term on the right-hand side of Eq.(4) vanishes for the two horizontal connecting legs if heat losses are neglected.

Equations (2) through (4) are the governing model equations in terms of the relevant parameters for each component of the loop. The most important parameters needing specifications for the solution of the problem are the friction factor f in the momentum equation, Eq. (3), and the overall heat transfer coefficient U_s for the source and sink in Eq.(4). Of course, the initial conditions and the temperature of the working fluid inside the tubes must also be known or calculable.

At steady-state conditions, the mass flow rate of the circulating fluid is constant. The integration of the momentum equation, Eq.(3), over each component of the loop and adding the equations results in the momentum equation for the entire loop,

$$(1/2\rho)G^2R = \rho_o g\beta \int_o^{L_s} [T_{so}(z) - T_{si}(z)dz/L_s = \rho_o g\beta L_s T_D \qquad (5)$$

where the effective flow resistance parameter R is composed of the sum of the frictional and form losses,

$$R = \sum_i \int_{s_i} (F_i/D_{hi}A_{fi})ds_i + \sum_j (K_j/A_{fj}^2) \qquad (6)$$

The momentum equation simply states that the frictional ppressure drop is balanced by the bouyancy forces.

Integration of the steady-state energy equation for each component of the loop and addition of the resulting equations yields an overall energy balance of the form

$$U_{so} A_{so} LMTD_{so} - U_{si} LMTD_{si}$$
$$= U_a P_a [L_L (\bar{T}_H + \bar{T}_C - 2T_a) + 2L_s LMTD_a] \qquad (7)$$

where LMTD denotes the logarithmic mean temperature difference. When Eq.(7) was written, it was assumed that the overall heat transfer coefficient between the circulating fluid and the ambient environment is independent of position along the loop. In this equation, the overall heat transfer coefficients in the source and sink are constant. This equation states that the heat input by the source is equal to the heat output by the sink plus the heat losses from the loop to the ambient environment.

3.3 Dynamic Response of System

When one integrates the momentum equation, Eq.(3), over each component and adds the resulting equations, the pressure term vanishes, and the momentum equation with the conservation of mass equation, Eq.(3), for flow in the loop becomes

$$\alpha \frac{dG}{dt} = -R \frac{1}{\rho} \frac{G^2}{2} + \rho_o g \beta L_s T_D \tag{8}$$

where α is the reciprocal of the flow area, A_f, integrated around the loop,

$$\alpha \equiv \int ds/A_f \tag{9}$$

The flow rate in the loop can be determined from Eq. (2) if the driving temperature, T_D, is known as a function of time.

With tube bundle #1 as the source and tube bundle #2 as the sink, integration of the energy equations, Eq.(4), over each component of the loop results in the following equations [11]:

$$\rho c_p V_{so} \frac{d\bar{T}_{so}}{dt} + G c_p | T_2 - T_1 | = Q_{so} - Q_{l_{so}} \tag{10a}$$

$$\rho c_p V_{si} \frac{d\bar{T}_{si}}{dt} + G c_p | T_4 - T_3 | = - Q_{si} - Q_{l_{si}} \tag{10b}$$

$$\rho c_p V_H \frac{d\bar{T}_H}{dt} + G c_p | T_3 - T_2 | = - Q_{l_H} \tag{10c}$$

$$\rho c_p V_C \frac{d\bar{T}_C}{dt} + G c_p | T_1 - T_4 | = - Q_l \tag{10d}$$

where the temperatures $\bar{T}_{so}$, $\bar{T}_{si}$, $\bar{T}_H$, and $\bar{T}_C$ are the average temperatures of the source, sink hot connecting leg, and cold connecting leg, respectively. The local temperatures T_1, T_2, T_3, and T_4 and the respective locations s_1, s_2, s_3, and s_4 are shown schematically in Figure 5. With the integrated average temperatures of each component expressed in terms of the four unknown local temperatures --T_1, T_2, T_3, and T_4--the resulting energy equations, Eqs. (10a) through (10d), along with the momentum Eq. (8) can be solved simultaneously for these four temperatures and the mass flow rate, G. This is possible if the heating rates -- Q_{so}, Q_{si}, and Q_l-- are known functions of time, determined by monitoring the heating and cooling fluid flow rates and temperature difference across the heat exchangers.

When one integrates the energy equations, Eq.(4), over each of the components, the second term on the right-hand side vanishes, and the resulting energy equation for the loop becomes

$$\rho_o c_p V \frac{d\bar{T}}{dt} = Q_{so} - Q_{si} - Q_l \qquad (11)$$

where $\bar{T}$ is the average temperature of the fluid in the loop. The energy balance, Eq.(11), states that the sum of the heat inflow from the source minus the heat outflow from the sink and the losses from the system to the ambient environment is equal to the time rate of change of the temperature of the system.

If the heat losses to the environment can be neglected, Eq.(11) reduces to

$$\rho_o c_p V \frac{d\bar{T}}{dt} = Q_{so} - Q_{si} \qquad (12)$$

The time rate of change of the average temperature in the loop can be determined from Eq. (12) if the differences in heat input and heat removal rates ae known function of time.

4. EXPERIMENTAL RESULTS AND DISCUSSION

4.1 Test Runs

The procedure outlined in Section 2.3.2 was followed in obtaining the experimental data of the steady-state test runs tabulated in Appendix A. The conditions of the system and the

relevant parameters were determined from this data. Details of the sample data reduction and experimental errors are given elsewhere [10]. Five different test runs were performed, and the major variations are given in Table 2. In each test run, tube bundle #1 acted as the source, and tube bundle #2 acted as the sink. In all tests, tube bundle #2 was in a counterflow arrangement.

Table 2. Steady-State Test Runs

Data Set	No. of Tests	$\dot{m}$ (kg/s) of Fluid Cooling	Heating	Heat Exchanger #1 Arrangement
A	15	0.06	0.3	Counterflow
B	15	0.03	0.3	Counterflow
C	15	0.09	0.3	Counterflow
D	16	0.06	0.2	Counterflow
E	16	0.06	0.3	Parallel Flow

Three different types of transient tests were performed: 1) the initial start-up Tr-1, 2) a step increase in heating fluid temperature Tr-2, and 3) a step decrease in heating fluid temperature Tr-3 are discussed here. In all three tests, both tube bundles were in a counterflow arrangement.

The presentation begins with a discussion of the steady-state flow and fluid friction results and then proceeds to an exposition of the results for steady-state heat transfer coefficients. The discussion concludes with a comparison between predicted and measured circulating fluid temperature under transient conditions.

4.2 Steady-State Mass Flow and Fluid Friction

The calculated heat losses to the ambient environment, the difference between the heat added by the source and the heat removed by the sink, were usually less than 10% of the heat added to the system. The error in measuring the heat added to the system was approximately equal to the values of the heat losses.

An average value for the heating rate was used to calculate the steady-state mass flow rates of the circulating fluid. Figure 5 illustrates the variation of heating rate Q with the flow rate G. As expected, the plot shows that higher rates of heat addition to the fluid in the loop result in higher in higher mass flow rates. It appears that changing the cooling fluid flow rate through the range of 0.03 to 0.09 kg/s does not affect the heating rate-flow rate relationship. Changing tube bundle #1 from a counterflow condition to a parallel-flow arrangement results in higher mass flow rates at equivalent heating rates. This is expected, since the driving temperature difference is higher at equivalent flow rate for the parallel-flow condition.

Flow was visualized with the dye tracer, and temperature traverses were made with the transversing thermocouple probe at the section of the hot connecting leg near the source. Because of the 90^{o}C bend, there was mixing, and the flow was turbulent in this section. A few centimeters downstream from the probes, the flow was observed to be laminar in the connecting legs. Flow separation and mixing at each corner section of the loop was expected.

For test set B at low cooling fluid flow rates, 0.03 kg/s, the average temperature of the fluid in the loop was higher than the other cooling fluid flow rates,k tests sets (A,C,D, and E). A plot of average temperature, $\bar{T}$, versus flow rate, G, is shown in Figure 6. Different average temperatures for equivalent flow rates indicate that variations in thermophysical properties should be accounted for in correlating the experimental results.

The Rayleigh number in free convection and the Reynolds number in forced convection are the major dimensionless parameters that were used to correlate the experimental results. In natural convection circulation systems, there is a combined effect of forced and free convection on heat transfer and fluid flow. The Rayleigh number dependence on the Reynolds number is illustrated in Figure 7. As the plot shows, the two parameters cannot be varied independently but have a definite relationship to each other. Test sets A through D are correlated by a least squares fit,

$$Ra = 575\ Re^{1.12}, \qquad 80 < Re < 650 \tag{13}$$

and test set E by

$$Ra = 769\ Re^{1.01}, \qquad 80 < Re < 480 \tag{14}$$

Both relations have a correlation coefficient of $r = 0.99$. The exponent on the Reynolds number term of approximately unity indicates that the Rayleigh number is almost directly proportional to the Reynolds number. This relationship should have been

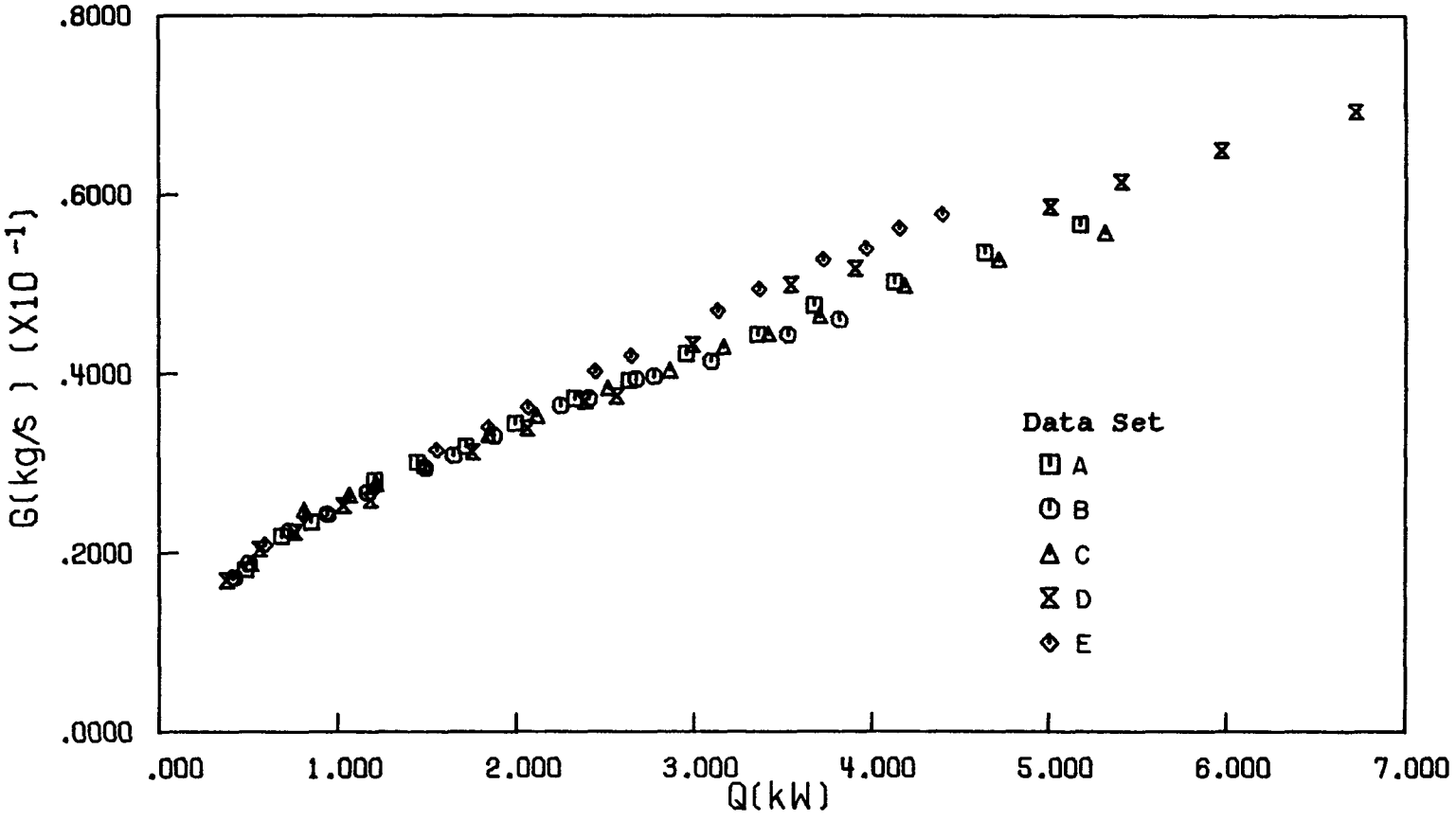

Figure 5. Variation of flow rate with heating rate.

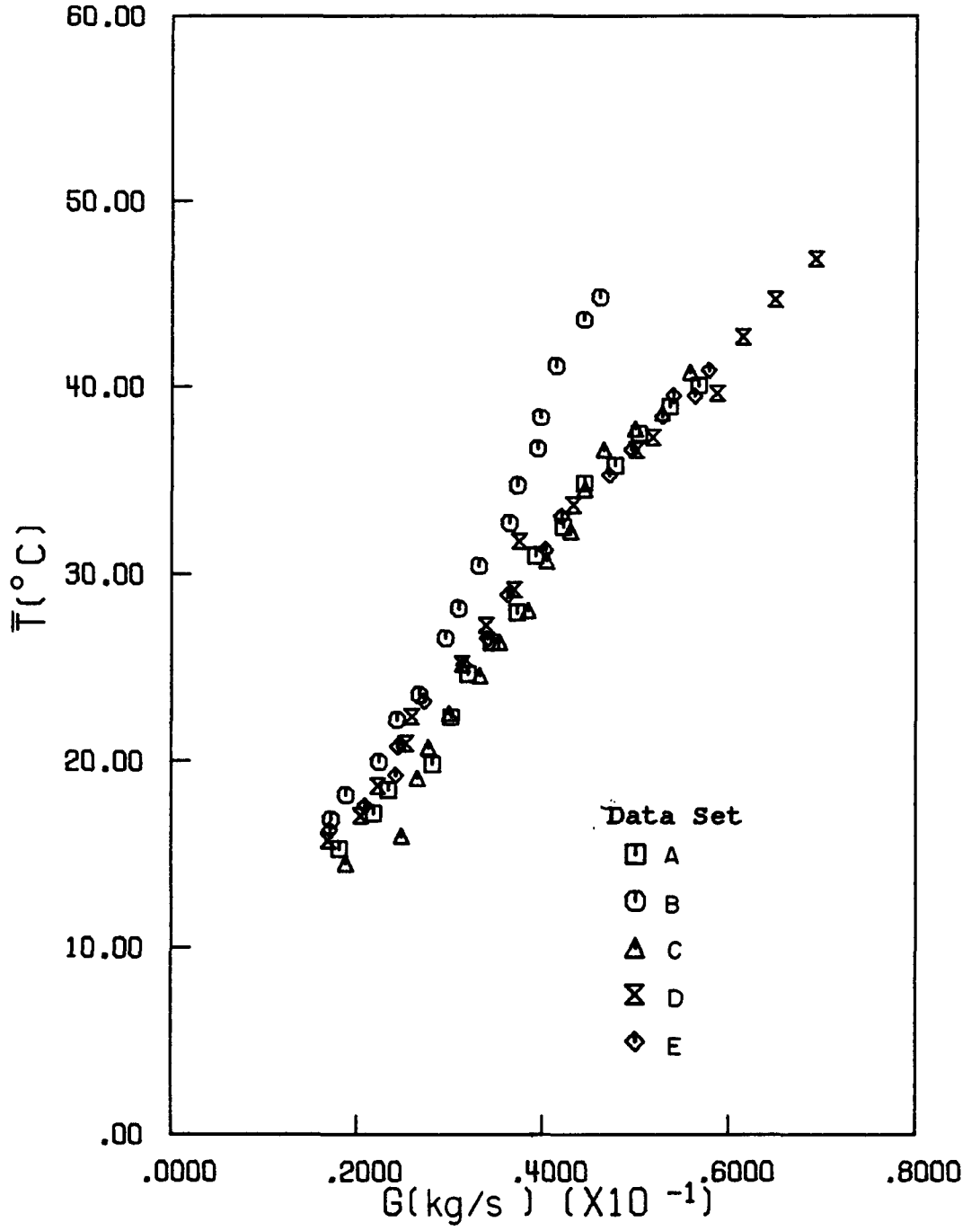

Figure 6. Variation of average temperature with flow rate.

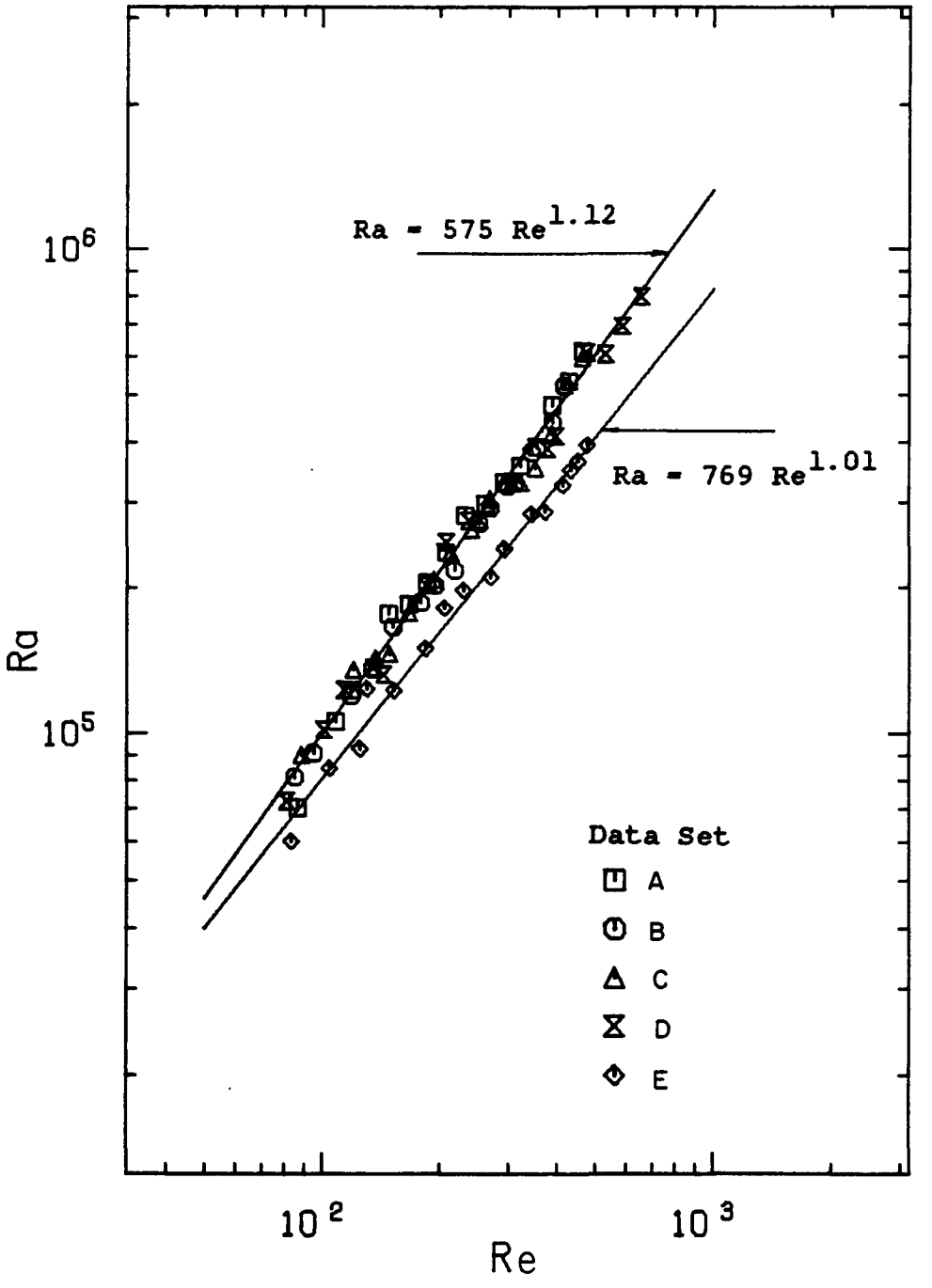

Figure 7. Rayleigh number dependence on Reynolds number.

anticipated from the results of Figure 5, which shows that for Q > 1 kW, the mass flow rate increases almost linearly with the power input into the system.

It was not feasible to determine the frictional pressure drop along the tube bundle. The static pressure difference along the bundle could have been measured, but because the fluid velocities were small, the dynamic pressure could not have been measured with sufficient accuracy. As a result, the frictional pressure drop could not be determined directly, and therefore an indirect method was employed to evaluate the total frictional resistance in the loop.

The analysis of the effective flow resistance parameter indicates that a plot of Ra_f^2 versus 1/Re would be a straight line of the form [11]

$$RA_f^2 = C_R/Re + K_T A_f^2 \qquad (15)$$

where, A_f and Re are the cross sectional flow area and the Reynolds number, respectively, in the section containing tube bundle #1. The constant C_R is composed of the individual friction factors for each loop component, and K_T is the total form loss coefficient for flow in the loop. Analysis of experimental data [10] has shown that C_R = 18,349 and $K_T A_f^2$ = -5. This indicates that the form losses in the loop have only a minor influence on the pressure drop around the loop, and the major factor controlling the frictional pressure drop is the first term on the right-hand side of Eq.(15). The form loss coefficient $K_T A_f^2$ was found to be small but negative by a least squares fit. This was due to experimental errors and the approximations used in calculating the driving temperature difference for determining the resistance parameter R. The major assumption made in determining the driving temperature difference was assuming the overall heat transfer coefficient to be constant along the length of the heat exchanger.

When numerical values for the hydraulic diameters, flow areas, and the lengths of the components are substituted from Table 1 and evaluated in equation (C-4), the constant C_R can be expressed as

$$C_R = 4a_L + 114\ a_1 + 161\ a_2 \qquad (16)$$

where a_1 , a_2 , and a_L are the individual friction factor coefficients in the Fanning friction factor relation, $f = a_L/Re^b$. Taking a_L = 16 and b = 1 [10] and assuming that $a_1 = a_2$, since the porosities are approximately equal [6], this yields a_1 = 66.5. Noting that 90% of the data lies in a range for C_R of

13,000 < C_R < 20,000, this gives a range for a_1 of 47 < a_1 < 72. The frictional pressure drop in the connecting legs for a_L = 16 is small compared with the pressure drop through the components containing the tube bundles.

The value of a_1 = 66.5 is only 5% higher than that predicted by the analysis of Zarling [7], which assumes fully developed laminar flow through a cluster of seven rods in a channel, similar to tube bundle #1. The experimental results for the friction factor constants, a_L, show little or no dependence on the Reynolds, Grashof, or Rayleigh numbers. This disagrees with the analysis of Yang [9], which shows a strong dependence on a Grashof-Reynolds number ratio for the pressure drop.

Expressing the resistance parameter as $R = C_R / \left[A_f^2 x\ Re \right]$ and by neglecting the form losses, one may rewrite the steady-state momentum equation, Eq.(13), in terms of a Grashof number Gr_{T_D} based on the the driving temperature, T_D , as

$$Gr_{T_D} \left[\frac{L_s}{D_h}\right] = C_R\ ARe/2 = \left[\frac{\rho^2 g\ \beta\ D_h^{\ 3}\ T_D}{\mu^2}\right] \left[\frac{L_s}{D_h}\right] \qquad (17)$$

A plot of $\log\left[Gr_{T_D}\ \left[L_s/D_h\right]\right]$ versus log Re revealed [11] that the data have a slope approximately equal to unity, indicating that the assumption of b = -1 in the friction factor relation is a reasonably good approximation.

4.3 Steady-State Average Heat Transfer Coefficients

The average Nusselt is based on the average convective heat transfer coefficient for heat transfer to the circulating fluid in the loop from the outside walls of tube bundle #1. The hydraulic diameter (D_h = 0.0138m) of the tube bundle is used. The thermopysical properties of water were evaluated at the average temperature of the fluid. The flow in the loop is driven by natural or forced. Since it has not been conclusively established in the literature what the appropriate correlating heat transfer parameters in a natural circulation loop should be, average Nusselt numbers are presented in terms of Reynolds, Rayleigh, and Grashof-to-Reynolds number ratio.

The effect of thermophysical property variations with temperature in correlating heat transfer results can be partially accounted by including the Prandtl number dependence on the Nusselt number. A plot of $\overline{Nu}/Pr^{0.43}$ versus Re is shown in Figure 8. Test sets A through D are correlated by a least squares fit of the form

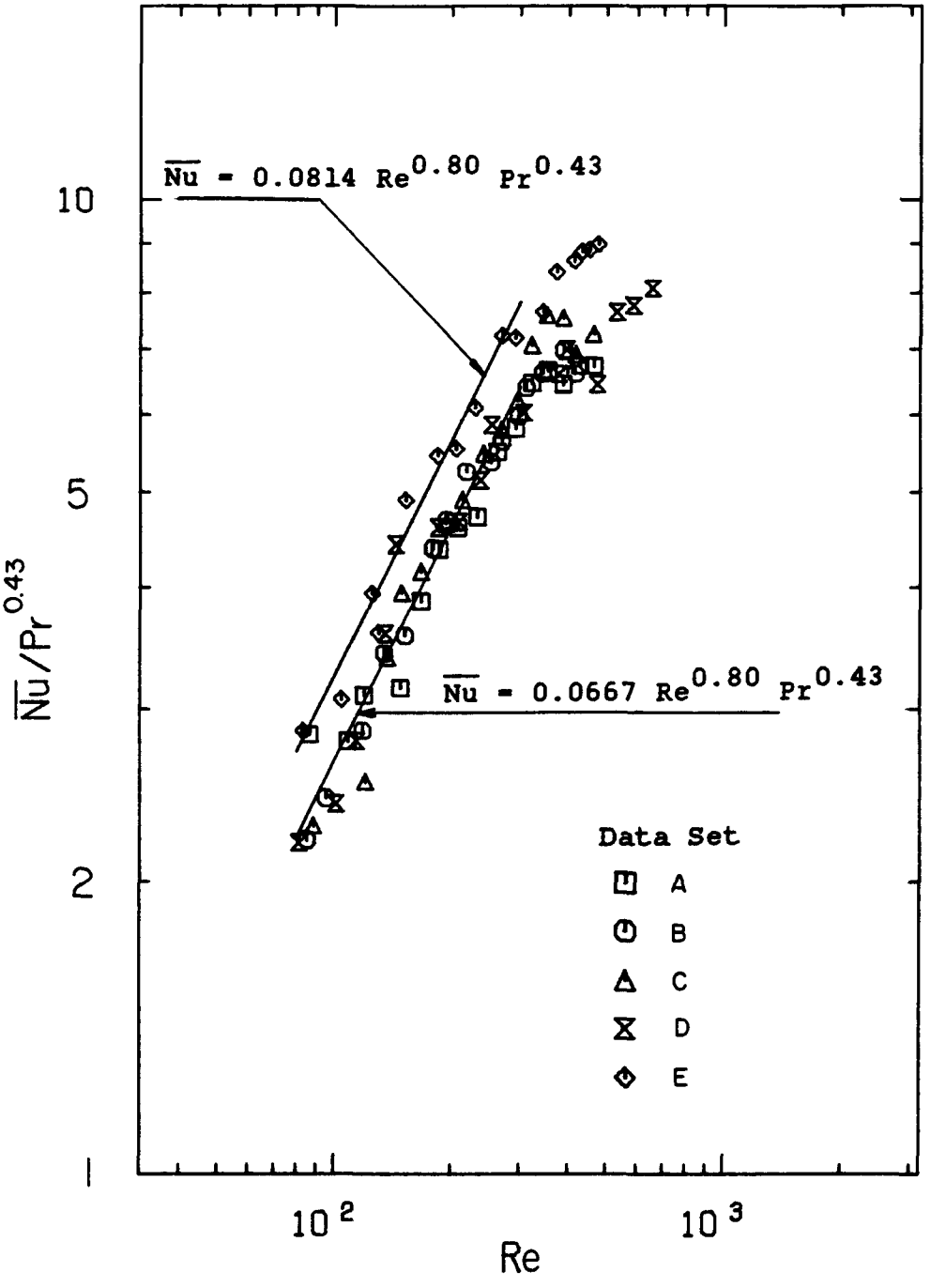

Figure 8. Heat transfer parameter dependence on Reynolds number.

$$\overline{Nu} = 0.0667\ Re^{0.80}\ Pr^{0.43}\ , \qquad 80 < Re < 300 \qquad (18)$$

and test set E is correlated by

$$\overline{Nu} = 0.0814\ Re^{0.80}\ Pr^{0.43}\ , \qquad 80 < Re < 300 \qquad (19)$$

For Re > 300, the average Nusselt number is overpredicted by Eqs. (18) and (19). Since the data are quite scattered, no correlation is given for Re > 300. The average Nusselt numbers are higher for test set E than for test sets A through D. This is expected, since higher flow rates have been obtained for equivalent heating rates. The results also show that there is poor correlation between the data for Re > 300, which indicates that the Reynolds number is not the only correlating parameter. The results suggest that secondary flow and mixing in the bundle may be possible reasons why the heat transfer coefficients are higher than what would be expected for laminar flow. An important feature of the flows in noncircular channels is the existence of secondary currents in the cross-sectional plane. As a result of these flows one would also expect circumferential variation in the heat transfer coefficient. The test bundle, however, was not instrumented for such detailed measurements. The results reported are for the circumferentially and longitudinalty averaged heat transfer coefficients.

Dwyer and Berry [8] have reported heat transfer results for fully developed forced convection laminar flow through a triangular array, with a pitch-to-diameter ratio of 1.25. This assumes fully developed flow and heat transfer with uniform heat flux along the length of the rod. For a uniform wall temperature boundary condition around the circumference of the rod, a value of 8.34 is reported for the Nusselt number; for the boundary condition of uniform wall heat flux around the circumference of the rod, a value of 7.97 is given. There is no Reynolds number dependence on the Nusselt number. The experimental results show that for Reynolds numbers greater than 130, their analytical results underpredict the heat transfer rates for natural circulation conditions.

For uniform heating, Subbotin, et al. [12] have obtained the following correlation for forced convection of water in a simulated infinite array with a pitch-to-diameter ratio of 1.2.

$$Nu = 0.025\ Re^{0.8}\ Pr^{0.43}\ , \qquad 500 < Re < 50{,}000 \qquad (20)$$

This empirical equation underpredicts the average Nusselt number. Entrance effects and strong secondary flows at the ends of the tube bundle could explain the higher heat transfer rates obtained from the present experimental measurements.

The dependence of the heat transfe parameter $\overline{Nu}/Pr^{0.43}$ on the Rayleigh number is shown in Figure 9. Test sets A through D are correlated by a least squares fit.

$$\overline{Nu} = 0.00116\ Ra^{0.67}\ Pr^{0.43}\ ,\ 60{,}000 < Ra < 500{,}000 \qquad (21)$$

and test set E,

$$\overline{Nu} = 0.00173\ Ra^{0.67}\ Pr^{0.43}\ ,\ 6x10^{4} < Ra < 5x10^{5} \qquad (22)$$

Again, for $Ra > 5x10^{5}$, Eq.(21) does not correlate the experimental data. The exponent on the Rayleigh number is approximately 2.5 times higher than that usually expected for laminar free convection conditions [10].

In our attempt to determine if heat transfer from the tube bundle to the fluid in the natural circulation loop behaves like combined forced and natural convection, the Grashof-to-Reynolds number ratio Gr/Re was used as a correlating parameter. The variation of $\overline{Nu}$ with Gr/Re is illustrated in Figure 10. Data sets A through D are correlated by a least squares fit,

$$\overline{Nu} = 0.0192\left[\frac{Gr}{Re}\right]^{1.2}\ ,\quad 75 < Gr/Re < 250 \qquad (23)$$

and data set E by

$$\overline{Nu} = 0.0191\left[\frac{Gr}{Re}\right]^{1.3}\ ,\quad 75 < Gr/Re < 250 \qquad (24)$$

For Gr/Re ratios above 250, the data points are quite scattered, and no meaningful least squares fits could be found. The combined convection heat transfer analysis in infinite rod arrays [9] has used the Gr/Re number ratio, where the Grashof number is based on an average heat flux along the length of the rod, as a correlating parameter. This Grashof-Reynolds number ratio is equivalent to $\overline{Nu}Gr/Re$. The analysis [9] only covers values of

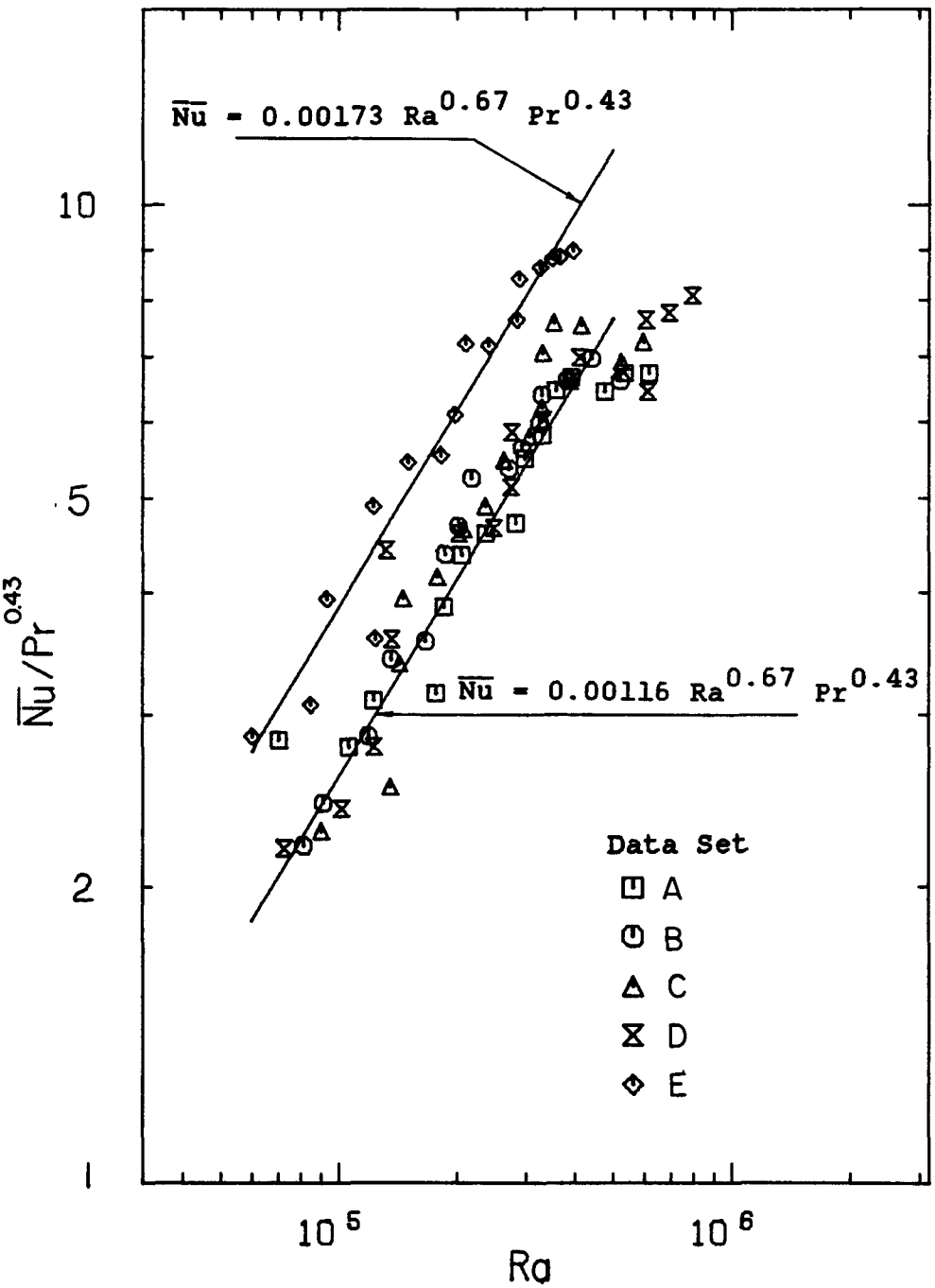

Figure 9. Average Nusselt number dependence on Rayleigh number.

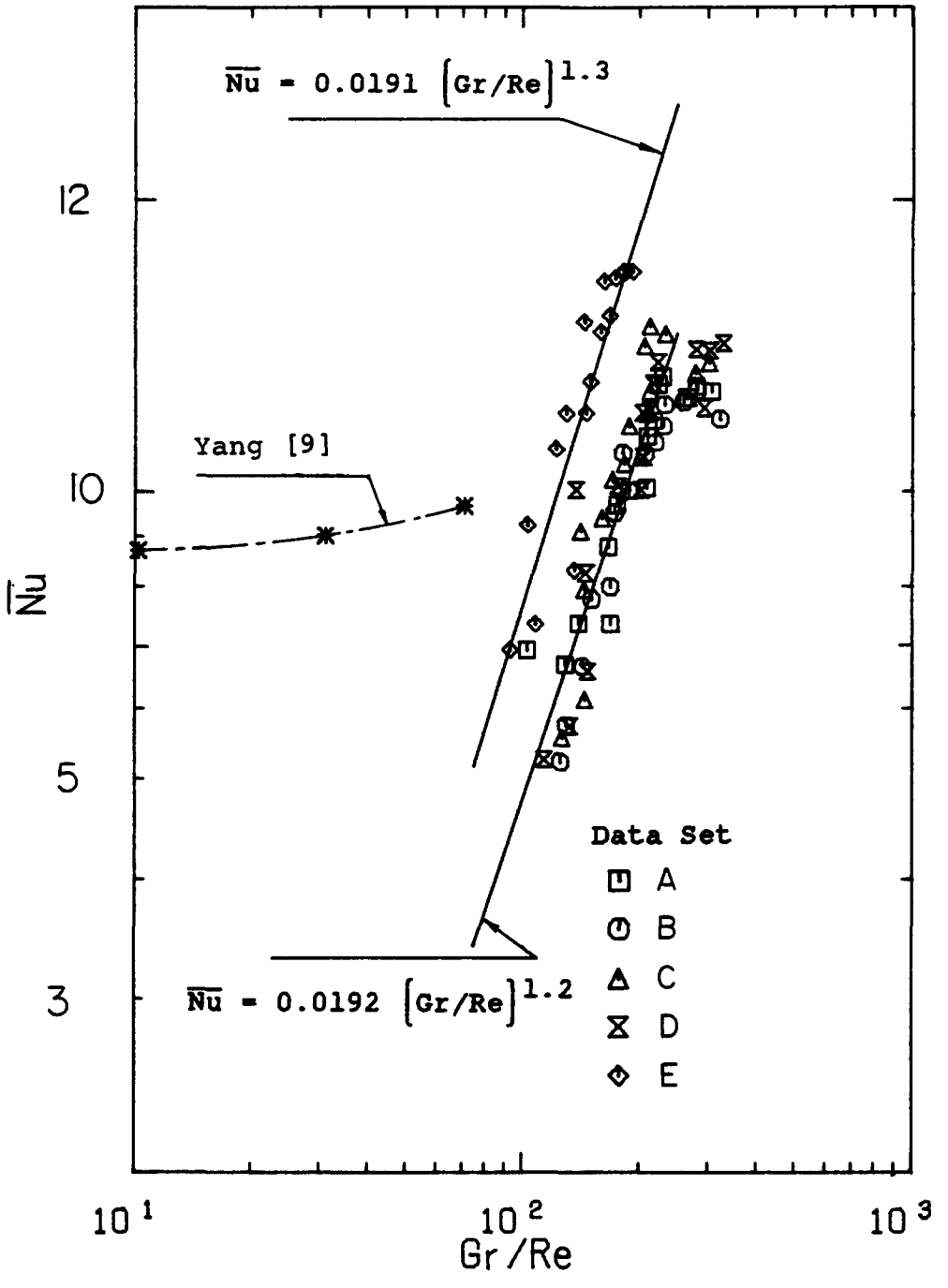

Figure 10. Heat transfer parameter dependence on Rayleigh number.

Gr/Re ratios up to 70($Gr\overline{Nu}/Re$ = 680), assuming fully developed flow and heat transfer with a constant heat flux along the length of the rod. The numerical results are outside the range of present experimental data but are included in Figure 10 for the purpose of comparison.

4.4 Comparison Between Measured and Predicted Dynamics Response of the Loop

The transient model equations, Eqs. (10a) through (10d), were solved for each component of the loop to predict the dynamic response of the natural circulation loop. The details can be found elsewhere [10]. It is sufficient to mention that the average temperature of the fluid in each component was expressed in terms of the local temperatures at the four corners of the loop. Heat exchanger theory was employed to obtain a local temperature variation along each component from which the average temperatures were determined. The bulk temperatures of the working fluids inside the heat exchangers were curve fitted to polynomial approximation and used in the expressions for the average temperatures for the source and sink components. The four energy equatons and the momentum equation were solved simultaneously by a Bashforth-Moulton predictor corrector method with a Runge-Kutta starter. The conditions for the three experiments selected for comparision are summarized in Table 3.

Table 3. Initial and Final Steady-State Conditions of the System for the Transient Tests: Mass Flow Rate of Heating Fluid, 0.27 kg/s; Mass Flow Rate of Cooling Period, 0.07 kg/s

Test	T_{hi} (°C)	Q (kW)	G (kg/s)	$\bar{T}_{so}$ (°C)	$\bar{T}_{si}$ (°C)
(Tr-1)					
Initial		0.000	0.0000	22.50	22.50
Final	27.46	0.858	0.0222	23.44	20.19
(Tr-2)					
Initial	27.46	0.858	0.0222	23.44	20.19
Final	45.76	2.647	0.0364	35.46	30.56
(Tr-3)					
Initial	45.76	2.656	0.0368	35.72	30.87
Final	27.96	1.140	0.0285	24.74	20.99

The local temperatures in the loop predicted by the analytical model for start-up test Tr-1 are compared with the experimentally measured temperatures in Figure 11. The predicted temperatures in the loop are bounded by the average temperatures inside the heat exchangers. The model fails to predict the local temperatues at the start of the transient, t < 1 minute, for two

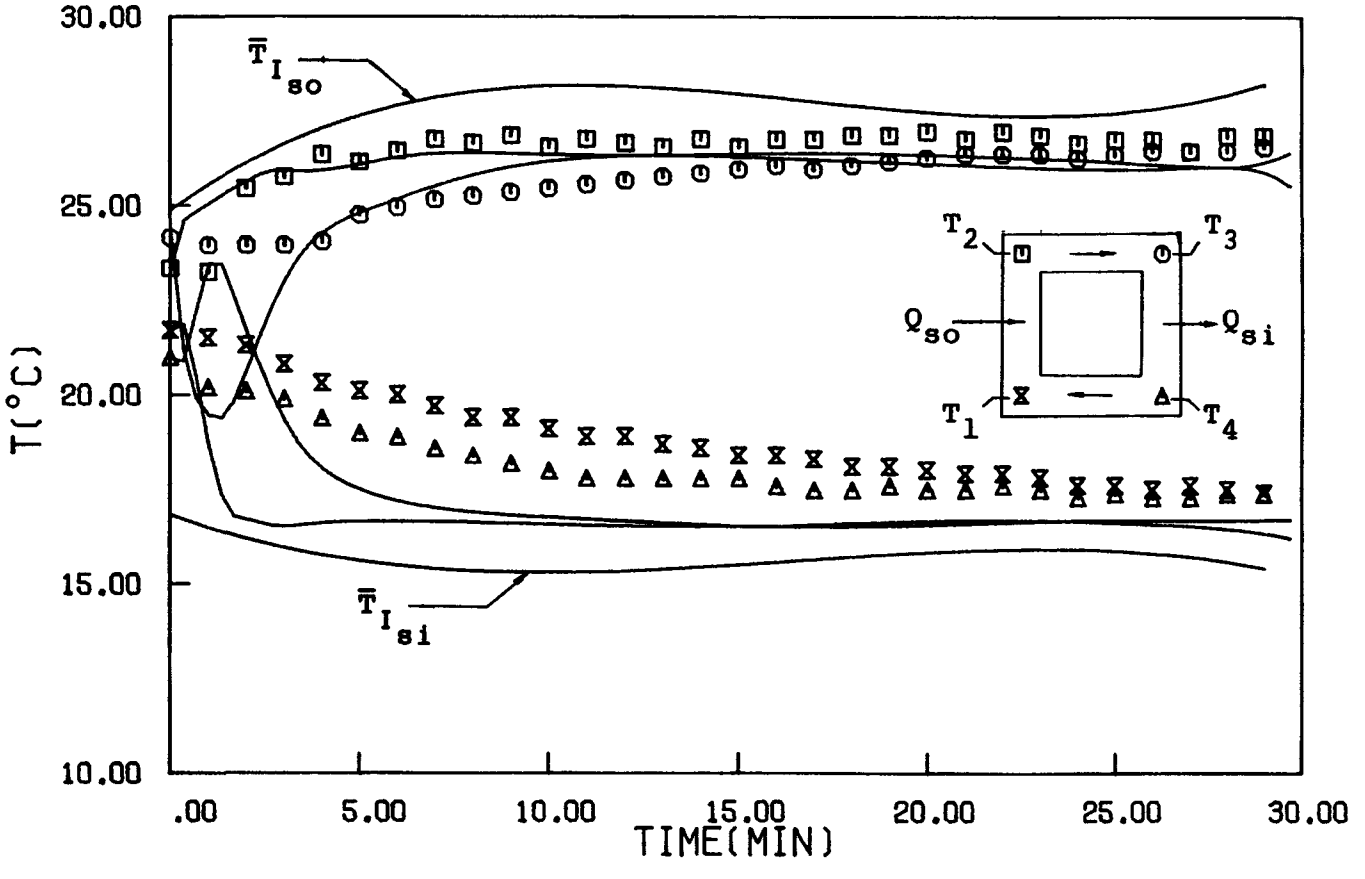

Figure 11. Local temperature variation with time in the loop for transient test Tr-1.

possible reasons: 1) the heat capacity of the loop and insulation is not accounted for and 2) the approximations for the average temperatures in the source and sink components do not hold for initial start up. After five minutes, when the heating and cooling rates are approximately equal and constant, the predicted local temperatures are almost invariant with time. The predicted flow rate [11] first shows a sharp increase in the rate, owing to the initially high driving temperature difference between the two vertical legs of the loop. It then decreases until it becomes constant as steady-state conditions are approached after about ten minutes. If a critical Rayleigh number for the onset of flow is included in the model, the flow rate would be zero until the buildup of buoyancy forces reached a critical value to overcome the frictional resistance. Then a sharp rise in the flow rate would occur sometime after t = 0.

Figure 12 shows the comparison between the predicted local temperatures and the measured temperatures for the step increase in heating fluid for experiment Tr-2. The model predicts the trends of the local temperatures fairly well but does not do so for the absolute values. This may possibly be due to the approximation used for the average temperatures in the connecting legs and the fact that the heat capacity of the structural components of the loop and the insulation are neglected. After twenty minutes, when the heating and cooling rates are approximately equal and constant, the predicted temperatures approach steady-state values. The model only predicts the general trends of the four local circulating fluid temperatures for transient experiments Tr-1 and Tr-3.

A comparison between the predicted and the measured average temperatures [$\bar{T} = (T_1 + T_2 + T_3 + T_4)/4$] in the loop is shown in Figure 13. The general trend of increasing average temperature is confirmed by the experimental data; however, the correct final steady-state value is confirmed for experiments Tr-1 and Tr-2 but not for Tr-3. For this latter test, the temperature of the heating fluid at the inlet of the heat exchanger was lowered, making the average temperature of the heating fluid inside the tube bundle lower than the average temperature of the fluid outside the tubes. This condition causes the heat to be removed by the source exchanger for approximately six minutes. After this, the overall heating rate to the system becomes positive, but the average temperature in the hot connecting leg is still higher than the temperature of the heating fluid inside the heating exchanger. In order to achieve a steady-state condition, the temperature of the fluid in the hot connecting leg must be lower than the temperature of the heating fluid inside the heat exchanger. At time t = 23 minutes, the calculated local temperature, T_3, is equal to the average temperature of the fluid inside the source tube bundle. This makes it difficult to evaluate the average temperature of the source.

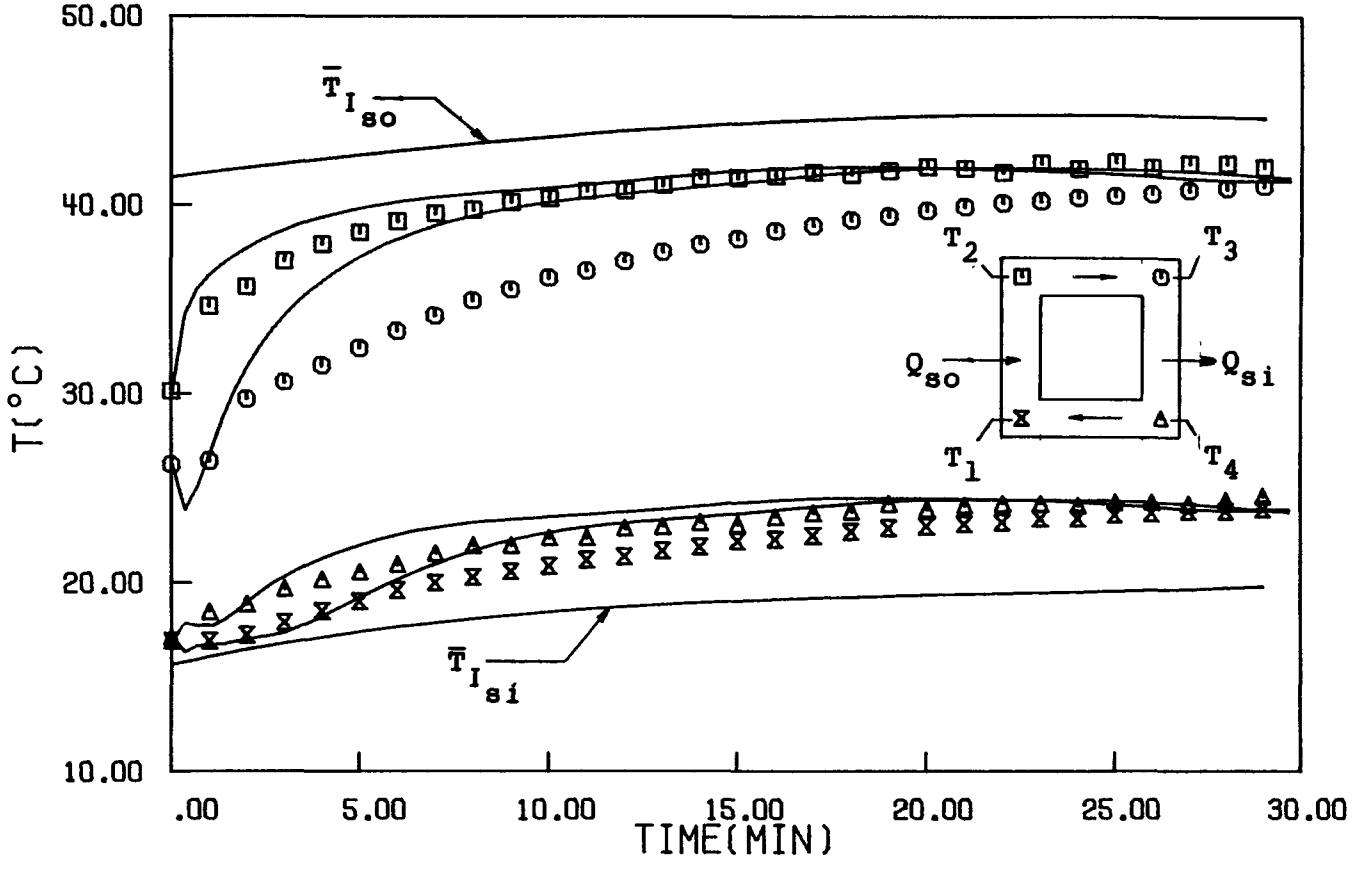

Figure 12. Local temperature variation with time in the loop for transient tests Tr-2.

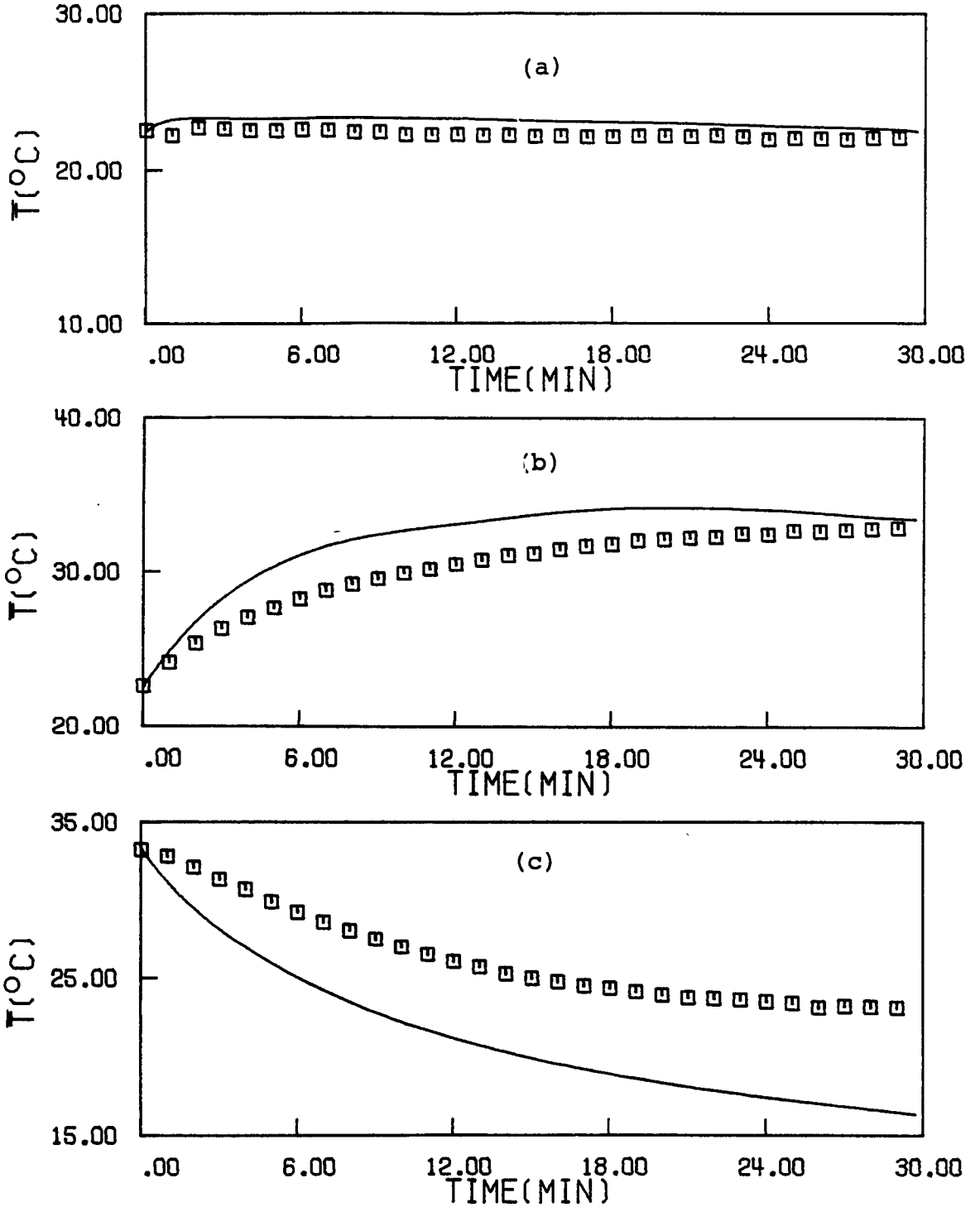

Figure 13. Variation of average temperature variation in the loop with time for the transient tests: (a) Tr-1, (b) Tr-2, (c) Tr-3.

The predicted mass flow rates for transient tests Tr-1 and Tr-2 first increase sharply because of the initial high driving temperature difference, $\overline{T}_D$, between the two vertical legs of the loop. They then decrease until they become constant as steady-state conditions are approached after about 10 minutes into the transient [11]. If the critical Rayleigh number for the onset of fluid flow was included in the model, the mass flow rate to the start-up transient test Tr-1 would be zero until the buildup of the buoyancy forces reached a critical value to overcome the frictional resistance. Then a sharp rise in flow rate would occur sometime after t = 0.

5. CONCLUSIONS AND RECOMMENDATIONS

5.1 Conclusions

Based on the experimental and analytical work reported, the conclusions of this study are:

1. The heating conditions investigated resulted in stable steady-state flows.

2. The parallel-flow arrangement of the source heat exchanger caused higher driving temperature differences, resulting in higher mass flow rates at equivalent heating rates than the counter-flow arrangement.

3. The frictional resistance was found to be dependent on the Reynolds number alone and seemed to be predicted well by forced flow correlations.

4. Nusselt numbers for natural convective circulation through the test tube bundle could not be predicted by laminar forced flow analysis but were dependent on heating rate, heat exchanger arrangement, and flow rate through the loop.

5. Higher local Nusselt numbers were obtained at the entrance region for natural circulation flow through the rod bundle.

6. The empirical correlations Eqs. (18) and (19) predicted the average Nusselt number most accurately. Since the heating rate of the fluid determines the magnitude of the mass flow rate of the fluid in the loop, one would expect a relation of this form to yield the best correlation.

7. The dynamics one-dimensional flow and the heat transfer model predicted only an approximate trend in the variation of local temperatures, mass flow rate, and average fluid temperature in the loop for the transient tests.

5.2 Recommendations

To advance understanding of longitudinal flow in a vertical tube bundle natural circulation conditions, the following areas are recommended for future investigation:

1. An extension of the present work to tube bundle geometries which are more prototypical of pressurized wter nuclear reactor fuel elements would be highly desirable.

2. Pressure drop measurements should be made to determine the friction factor dependence on flow conditions.

3. A more suitable method should be developed to determine the local heat transfer coefficients in the entrance regions for flow through tube bundles.

4. An analysis of the velocity and temperature distribution around vertical rod arrays should be undertaken to predict fluid flow and heat transfer under natural circulation conditions.

5. The dynamic one-dimensional flow and heat-transfer model should be modified in order to obtain improved agreement between predictions and experimental data.

APPENDIX A

Table 4. Steady-State Experimental Data

Test No.	$\dot{m}_1$ (kg/s)	T_{i_1} (^{o}C)	ΔT_1 (^{o}C)	$\dot{m}_2$ (kg/s)	T_{i_2} (^{o}C)	ΔT_2 (^{o}C)	$\overline{T}_H$ (^{o}C)	$\overline{T}_C$ (^{o}C)	$\overline{T}_w$ (^{o}C)
A-1	0.3352	19.37	0.39	0.0600	11.79	1.66	18.65	12.32	18.51
A-2	0.3309	22.72	0.54	0.0599	12.10	2.43	21.02	21.02	13.60
A-3	0.3246	25.03	0.67	0.0598	12.15	3.17	22.87	14.20	23.36
A-4	0.3271	28.30	0.97	0.0598	12.57	4.24	25.17	15.00	26.26
A-5	0.3380	31.16	1.10	0.0595	12.85	5.33	28.20	16.72	29.13
A-6	0.3308	34.43	1.31	0.0597	13.62	6.45	31.08	18.28	32.00
A-7	0.3279	37.16	1.51	0.0598	13.77	7.61	33.23	19.39	34.46
A-8	0.3331	39.90	1.77	0.0599	14.27	8.70	35.44	20.51	37.12
A-9	0.3283	43.52	2.00	0.0599	14.82	10.09	38.95	22.89	40.26
A-10	0.3308	45.66	2.28	0.0599	15.30	10.97	40.90	24.17	42.37
A-11	0.3343	48.94	2.43	0.0598	15.12	13.22	43.62	25.57	45.43
A-12	0.3363	50.52	2.74	0.0601	15.52	13.90	44.91	26.49	46.73
A-13	0.3267	54.03	3.12	0.0606	16.09	15.77	47.14	27.52	50.13
A-14	0.3280	56.95	3.55	0.0604	15.99	17.39	49.24	28.56	52.44
A-15	0.3327	59.87	3.91	0.0611	16.14	19.24	50.96	29.12	55.07
B-1	0.3314	20.63	0.36	0.0329	13.10	2.41	19.96	14.20	19.93
B-2	0.3325	22.53	0.41	0.0325	13.60	3.12	21.52	15.17	21.62
B-3	0.3263	25.39	0.62	0.0323	13.65	4.60	24.05	16.27	24.33
B-4	0.3316	28.42	0.77	0.0319	14.00	6.09	26.98	17.73	27.00
B-5	0.3344	31.11	0.90	0.0318	14.00	8.04	28.81	18.40	29.45
B-6	0.3287	34.91	1.15	0.0320	14.20	10.29	32.51	20.51	32.90
B-7	0.3296	36.97	1.28	0.0320	14.50	11.39	34.48	21.76	34.83
B-8	0.3330	39.78	1.41	0.0315	15.25	13.50	37.04	23.53	37.46
B-9	0.3317	43.40	1.72	0.0316	15.60	15.92	39.95	25.22	40.80
B-10	0.3285	45.92	1.84	0.0311	16.49	17.53	42.27	26.81	43.14
B-11	0.3298	48.77	2.02	0.0312	16.99	19.64	44.58	28.32	45.71
B-12	0.3318	50.31	2.07	0.0305	17.56	20.95	46.39	29.68	47.36
B-13	0.3322	54.13	2.25	0.0300	17.91	24.37	49.61	31.74	51.05
B-14	0.3336	57.25	2.64	0.0295	18.06	27.37	52.72	33.71	54.20
B-15	0.3342	59.62	2.89	0.0289	18.40	29.61	54.43	34.63	56.63

Table 4. (Continued)

C-1	0.3294	19.37	0.41	0.0843	11.22	1.26	17.98	11.57	18.31
C-2	0.3258	22.40	0.69	0.0864	11.52	1.87	20.18	12.37	21.09
C-3	0.3289	26.15	0.85	0.0868	12.55	2.64	24.07	14.50	24.70
C-4	0.3300	28.10	0.95	0.0866	12.72	3.07	26.05	15.62	26.44
C-5	0.3280	31.11	1.15	0.0863	13.17	3.83	28.56	16.72	29.28
C-6	0.3329	34.36	1.41	0.0862	13.35	4.77	31.30	18.03	32.03
C-7	0.3295	37.07	1.61	0.0862	13.70	5.54	33.54	19.24	34.46
C-8	0.3336	39.85	1.92	0.0860	13.80	6.50	35.94	20.33	36.82
C-9	0.3297	43.64	2.20	0.0862	14.32	7.44	39.24	22.30	40.24
C-10	0.3342	45.87	2.41	0.0861	14.75	8.22	41.14	23.53	42.22
C-11	0.3311	48.45	2.56	0.0861	15.35	9.10	43.59	25.27	44.43
C-12	0.3343	50.98	2.71	0.0866	15.77	9.99	45.99	26.93	46.86
C-13	0.3344	53.62	3.09	0.0860	15.47	11.22	47.65	27.61	49.13
C-14	0.3250	56.97	3.65	0.0862	15.47	12.37	49.26	27.88	52.05
C-15	0.3295	60.71	3.99	0.0862	15.84	14.22	52.09	29.32	55.59

D-1	0.2395	19.76	0.41	0.0598	12.90	1.38	18.60	13.22	18.83
D-2	0.2350	22.48	0.64	0.0600	13.35	1.97	20.60	14.00	20.98
D-3	0.2268	25.39	0.85	0.0582	13.60	2.94	22.92	14.77	23.48
D-4	0.2372	28.54	1.08	0.0594	13.40	3.99	25.86	16.12	26.19
D-5	0.2314	30.33	1.26	0.0582	13.40	4.72	27.83	16.94	27.63
D-6	0.2336	34.29	1.92	0.0597	13.05	6.50	31.91	18.55	32.48
D-7	0.2352	37.78	2.23	0.0596	13.90	7.74	34.58	20.04	35.49
D-8	0.2350	40.57	2.61	0.0595	14.40	8.88	36.95	21.49	37.93
D-9	0.2354	43.26	2.66	0.0595	15.30	10.06	39.74	23.39	40.71
D-10	0.2355	45.43	3.20	0.0595	16.12	11.39	41.85	25.32	43.55
D-11	0.2363	49.31	3.68	0.0589	16.54	14.00	44.89	27.93	47.25
D-12	0.2406	50.61	4.04	0.0586	15.07	15.30	46.13	28.08	48.47
D-13	0.2357	57.20	5.26	0.0601	15.17	19.20	49.73	29.34	54.61
D-14	0.2352	59.94	5.79	0.0597	15.69	20.51	53.09	32.03	56.75
D-15	0.2382	63.27	6.20	0.0599	16.52	23.04	55.48	33.50	60.13
D-16	0.2400	67.20	7.08	0.0597	16.89	25.42	58.41	35.18	63.62

Table 4. (Continued)

E-1	0.3269	20.06	0.31	0.0584	12.77	1.59	19.15	13.50	19.29
E-2	0.3288	22.33	0.46	0.0593	13.10	2.23	21.05	14.25	21.47
E-3	0.3310	24.66	0.62	0.0586	13.15	3.09	23.19	15.22	23.45
E-4	0.3292	27.57	0.67	0.0589	13.37	3.91	25.20	15.99	26.15
E-5	0.3291	30.36	0.85	0.0585	13.65	5.03	28.22	17.68	28.79
E-6	0.3247	33.23	1.15	0.0579	13.82	6.32	30.79	19.02	31.50
E-7	0.3261	35.63	1.38	0.0569	13.80	7.51	32.75	19.84	33.78
E-8	0.3338	38.52	1.51	0.0587	14.72	8.22	35.39	21.76	36.42
E-9	0.3272	41.51	1.82	0.0585	15.40	9.81	38.21	23.70	39.17
E-10	0.3299	43.92	1.97	0.0584	15.97	10.54	40.28	25.20	41.51
E-11	0.3335	47.21	2.28	0.0582	16.24	12.67	42.79	26.88	44.60
E-12	0.3360	48.56	2.48	0.0584	16.69	13.25	44.37	28.10	45.91
E-13	0.3276	51.05	2.84	0.0579	16.96	14.70	46.44	29.56	48.40
E-14	0.3215	52.95	2.99	0.0603	16.76	15.52	47.82	30.24	50.13
E-15	0.3264	53.02	3.20	0.0602	16.76	15.72	47.96	30.29	50.37
E-16	0.3264	55.46	3.27	0.0603	16.81	17.16	49.47	31.28	52.20

APPENDIX B

Table 5. Calculted Steady-State Experimental Results

Test No.	Q (kW)	G (kg/s)	$Rx10^{-4}$ (m^{-4})	T_D ($^{\circ}C$)	Re	$\overline{Nu}$	Pr	$Grx10^{-3}$	$Rax10^{-3}$
A-1	0.48	0.0181	3890.0	2.41	86.	6.88	7.93	8.86	70.3
A-2	0.68	0.0218	2136.0	1.93	108.	6.64	7.58	13.9	105.4
A-3	0.85	0.0234	2051.0	2.13	119.	7.32	7.36	16.6	122.2
A-4	1.20	0.0281	1653.0	2.48	148.	7.32	7.09	24.9	176.5
A-5	1.44	0.0301	1554.0	2.67	166.	8.76	6.69	27.6	184.6
A-6	1.71	0.0319	1399.0	2.71	186.	9.67	6.33	32.4	205.1
A-7	1.99	0.0344	1210.0	2.72	207.	10.00	6.08	38.9	236.5
A-8	2.32	0.0372	1129.0	2.97	232.	10.07	5.84	48.3	282.1
A-9	2.63	0.0392	975.2	2.86	262.	11.38	5.43	54.8	297.6
A-11	3.35	0.0444	832.3	3.14	322.	12.86	4.96	71.9	356.6
A-12	3.67	0.0477	718.3	3.13	354.	13.09	4.82	81.0	390.4
A-13	4.12	0.0503	608.7	2.96	387.	12.46	4.64	102.5	475.6
A-14	4.63	0.0536	544.4	3.00	428.	12.80	4.46	119.5	533.0
A-15	5.17	0.0567	480.7	2.97	464.	12.64	4.34	141.7	615.0
B-1	0.42	0.0172	2712.0	1.52	85.	5.28	7.63	10.6	80.9
B-2	0.50	0.0188	2296.0	1.53	95.	5.75	7.39	12.3	90.9
B-3	0.73	0.0224	1900.0	1.81	118.	6.61	7.07	16.8	118.8
B-4	0.94	0.0243	1579.0	1.77	134.	7.75	6.70	20.2	135.3
B-5	1.16	0.0267	1527.0	2.07	152.	7.98	6.50	25.5	165.8
B-6	1.48	0.0295	1230.0	2.04	179.	9.50	6.05	30.8	186.3
B-7	1.64	0.0309	1194.0	2.17	194.	9.97	5.81	34.8	202.2
B-8	1.87	0.0331	1022.0	2.14	218.	10.93	5.51	39.5	217.6
B-9	2.24	0.0364	824.0	2.08	252.	10.92	5.21	52.1	271.4
B-10	2.40	0.0372	799.9	2.12	269.	11.22	4.96	59.0	292.6
B-11	2.67	0.0394	735.5	2.18	297.	11.67	4.74	68.3	323.7
B-12	2.77	0.0397	694.0	2.10	311.	12.27	4.56	72.0	328.3
B-13	3.09	0.0414	586.4	1.93	343.	12.35	4.28	88.8	380.1
B-14	3.52	0.0444	490.0	1.86	389.	12.68	4.02	109.4	439.8
B-15	3.81	0.0461	429.0	1.75	415.	11.86	3.90	133.4	520.3

Table 5. (Continued)

C-1	0.51	0.0188	3346.0	2.24	88.	5.59	8.06	11.1	89.5
C-2	0.81	0.0248	2008.0	2.33	120.	6.11	7.78	17.3	134.6
C-3	1.06	0.0265	2010.0	2.67	137.	7.93	7.23	19.7	142.4
C-4	1.21	0.0277	1843.0	2.69	148.	9.09	6.96	20.9	139.8
C-5	1.48	0.0299	1738.0	2.96	166.	9.38	6.66	26.6	177.2
C-6	1.84	0.0332	1428.0	2.99	193.	10.27	6.33	32.8	207.6
C-7	2.11	0.0353	1276.0	3.02	213.	10.66	6.07	38.9	236.1
C-8	2.51	0.0384	1186.0	3.33	241.	11.67	5.81	45.4	263.8
C-9	2.86	0.0404	1065.0	3.31	269.	12.01	5.45	56.0	305.2
C-10	3.16	0.0430	958.4	3.38	296.	12.65	5.24	62.8	329.1
C-11	3.41	0.0445	917.3	3.48	321.	14.09	4.98	66.3	330.2
C-12	3.70	0.0465	842.0	3.49	351.	14.79	4.73	74.7	353.3
C-13	4.18	0.0499	727.9	3.48	387.	14.51	4.60	90.2	414.9
C-14	4.71	0.0528	655.4	3.50	418.	13.20	4.50	116.3	523.4
C-15	5.31	0.0558	597.7	3.57	463.	13.53	4.27	139.6	596.1
D-1	0.38	0.0169	3686.0	1.98	81.	5.31	7.85	9.24	72.5
D-2	0.56	0.0204	2630.0	2.07	101.	5.74	7.59	13.4	101.7
D-3	0.76	0.0223	2425.0	2.28	114.	6.54	7.30	16.8	122.6
D-4	1.03	0.0253	1797.0	2.18	136.	8.24	6.93	19.7	136.5
D-5	1.18	0.0259	1866.0	2.39	144.	10.02	6.70	19.7	132.0
D-6	1.75	0.0313	1585.0	2.96	184.	10.11	6.24	32.4	202.2
D-7	2.06	0.0339	1306.0	2.85	209.	10.02	5.93	41.9	248.5
D-8	2.38	0.0369	1158.0	3.01	237.	10.83	5.66	48.7	275.6
D-9	2.56	0.0375	1190.0	3.19	254.	12.04	5.34	51.8	276.6
D-10	2.99	0.0433	862.4	3.09	307.	12.12	5.08	65.2	331.2
D-11	3.54	0.0500	531.3	2.54	377.	12.89	4.74	81.8	387.7
D-12	3.90	0.0518	562.5	2.89	396.	13.55	4.66	88.3	411.5
D-13	5.00	0.0587	374.8	2.48	475.	12.17	4.39	139.2	611.1
D-14	5.40	0.0615	361.0	2.62	531.	13.98	4.09	148.4	607.0
D-15	5.97	0.0650	293.3	2.39	585.	13.94	3.91	177.5	694.0
D-16	6.72	0.0693	273.1	2.53	655.	14.19	3.70	215.3	796.6

Table 5. (Continued)

E-1	0.41	0.0171	3688.0	2.05	83.	6.88	7.77	7.73	60.1
E-2	0.59	0.0209	2783.0	2.30	104.	7.31	7.52	11.2	84.2
E-3	0.81	0.0242	2221.0	2.46	125.	9.23	7.24	12.8	92.7
E-4	0.94	0.0244	2167.0	2.45	130.	8.29	7.00	17.6	123.2
E-5	1.20	0.0272	2003.0	2.81	152.	11.04	6.60	18.5	122.1
E-6	1.55	0.0315	1699.0	3.20	184.	12.02	6.29	23.8	149.7
E-7	1.84	0.0340	1559.0	3.43	205.	12.03	6.08	29.9	181.8
E-8	2.06	0.0362	1350.0	3.38	230.	12.94	5.75	34.3	197.2
E-9	2.44	0.0403	1192.0	3.69	269.	14.93	5.42	38.8	210.3
E-10	2.64	0.0420	1068.0	3.59	292.	14.58	5.19	46.3	240.3
E-11	3.13	0.0471	861.6	3.65	343.	15.16	4.93	57.6	284.0
E-12	3.36	0.0495	823.5	3.86	372.	16.45	4.76	60.4	287.5
E-13	3.72	0.0528	733.0	3.92	412.	16.57	4.56	71.4	325.6
E-14	3.96	0.0540	696.4	3.90	432.	16.76	4.45	78.5	349.3
E-15	4.15	0.0563	683.9	4.16	451.	16.83	4.44	82.2	365.0
E-15	3.39	0.0578	591.1	3.79	476.	16.84	4.31	91.5	394.4

ACKNOWLEDGEMENTS

This work was sponsored by the U.S. Nuclear Regulatory Commission through a subcontract from Argonne National Laboratory. The authors are indebted to Dr. Paul A. Lottes for many helpful discussions. Except for revisions and condensation, this report constitutes the MSME Thesis of Michael J. Gruszczynski.

REFERENCES

1. Japikse, D., "Advances in Thermosyphon Technology," in Advances in Heat Transfer, Vol. 9, Academic Press, New York, 1973, pp. 1-111.

2. Zvirin, Y., "A Review of Natural Circulation Loops in Pressurized Water Reactors and Other Systems," Electric Power Research Institute Report No. NP-1676-SR, Palo Alto, Calif., January 1981.

3. Mertol, A., Place, W., Webster, T., and Greif, R., "Detailed Loop Model (DLM) Analysis of Liquid Solar Thermosyphons with Heat Exchangers," Lawrence Berkeley Laboratory Report LBL-10699, October 1980.

4. Viskanta, R. and Mohanty, A.K., "TMI-2 Accident: Postulated Heat Transfer Mechanisms and Available Data Base," Argonne National Laboratory Report ANL-81-26 (NUREG/CR-2121), April 1981.

5. Tong, L.S. and Weisman, J., Thermal Analysis of Pressurized Water Reactors, Second Edition, The American Nuclear Society, Hinsdale, Illinois, 1979.

6. Sparrow, E.M. and Loeffler, A.L., "Longitudinal Laminar Flow Between Cylinders Arranged in Regular Arrays," AIChE Journal, Vol.5, pp. 325-330, 1959.

7. Zarling, J.P., "Laminar-Flow Pressure Drop in Symmetrical Finite Rod Bundles," Nuclear Science and Engineering, Vol.61, pp. 282-285, 1976.

8. Dwyer, O.E. and Berry, H.C., "Laminar-Flow Heat Transfer for In-Linnne Flow Through Unbaffled Rod Bundles," Nuclear Science and Engineering, Vol.42, pp. 81-85, 1970.

9. Yang, J.M., "Analysis of Combined Convection Heat Transfer in Infinite Rod Arrays," in Heat Transfer 1978, Vol.1, National Research Concil of Canada, Ottawa, 1979, pp. 49-54.

10. Incropera, F.P. and DeWitt, D.P., Fundamentals of Heat Transfer, Wiley Book Co., New York, 1981.

11. Grusczynski, M.J., "Heat Transfer from a Vetical Tube Bundle under Natural Circulation Conditions," MSME thesis, Purdue University, August 1982.

12. Rohsenow, W.H. and Hartnett, J.P., eds., Handbook of Heat Transfer, McGraw-Hill Book Co., New York, 1973, p.7-134.

Distribution for NUREG/CR-3167 (ANL-83-7)

Internal:

E. S. Beckjord
C. E. Till
R. Avery
B. R. T. Frost
P. A. Lottes (10)
ANL Patent Dept.
ANL Contract File
ANL Libraries (2)
TIS Files (6)

External:

NRC, for distribution per R2 and R4 (395)
DOE-TIC, Oak Ridge (2)
Manager, Chicago Operations Office, DOE
Chief, Office of Patent Counsel, DOE-CH
Reactor Analysis and Safety Division Review Committee:
W. P. Chernock, Combustion Engineering, Inc., 1000 Prospect Hill Road, Windsor, Conn. 06095
L. C. Hebel, Xerox Corp., 333 Coyote Hill Road, Palo Alto, Calif. 94304
S. Levine, NUS Corp., 910 Clopper, Gaithersburg, Md. 20878
W. F. Miller, Jr., Los Alamos National Laboratory, P. O. Box 1663, Los Alamos, N. Mex. 87545
M. J. Ohanian, College of Engineering University of Florida, Gainesville, Fla. 32611
T. H. Pigford, College of Engineering, University of California - Berkeley, Berkeley, Calif. 94720
J. J. Taylor, Electric Power Research Institute, P. O. Box 10412, Palo Alto, Calif. 94303
R. Viskanta, Purdue University, West Lafayette, Ind. 47907 (10)

NRC FORM 335 (11-81) U.S. NUCLEAR REGULATORY COMMISSION

BIBLIOGRAPHIC DATA SHEET

1 REPORT NUMBER (Assigned by DDC)
NUREG/CR-3167

4 TITLE AND SUBTITLE (Add Volume No., if appropriate)
HEAT TRANSFER TO WATER FROM A VERTICAL TUBE BUNDLE UNDER NATURAL CIRCULATION CONDITIONS

2 (Leave blank)

3 RECIPIENT'S ACCESSION NO
ANL-83-7

7 AUTHOR(S)
M. J. Gruszczynski and R. Viskanta

5. DATE REPORT COMPLETED
MONTH: August YEAR: 1982

DATE REPORT ISSUED
MONTH: January YEAR: 1983

9 PERFORMING ORGANIZATION NAME AND MAILING ADDRESS (Include Zip Code)
School of Mechanical Engineering
Purdue University
West Lafayette, Indiana 47907

6 (Leave blank)

8 (Leave blank)

12 SPONSORING ORGANIZATION NAME AND MAILING ADDRESS (Include Zip Code)
Argonne National Laboratory
9700 South Cass Avenue
Argonne, Illinois 60439

10. PROJECT/TASK/WORK UNIT NO

11 FIN NO
A2014

13 TYPE OF REPORT
Technical Report

PERIOD COVERED (Inclusive dates)

15 SUPPLEMENTARY NOTES

14 (Leave blank)

16 ABSTRACT (200 words or less)

A rectangular natural circulation loop (thermosyphon) was used to measure the average heat transfer coefficients under natural convection conditions of water at atmospheric pressure from a vertical tube bundle. A seven tube bundle having a pitch-to-diameter tube ratio of 1.25 was used as a test heat exchanger. A circulating flow was established in the loop by the buoyancy differences in its two vertical legs. Steady state tests yielded empirical relations between the dimensionless parameters that govern fluid flow and heat transfer in the system. Empirical correlations for average Nusselt number are reported. A one-dimensional, transient model was developed and used to predict the temperatures and flow rates under natural circulation conditions. The model was not able to predict correctly the early transient respose but yielded correct results for the steady state conditions at the end of the transient.

17 KEY WORDS AND DOCUMENT ANALYSIS

17a DESCRIPTORS

Heat transfer coefficient
Natural convection circulation
Natural convection heat transfer
Rectangular loop
Transient response of a natural circulation loop
Vertical tube bundle

17b IDENTIFIERS OPEN ENDED TERMS

18 AVAILABILITY STATEMENT
Unlimited

19 SECURITY CLASS (This report)
Unclassified

21 NO OF PAGES

20 SECURITY CLASS (This page)

22 PRICE
S

NRC FORM 335 (11-81)